

# Reach-avoid games for players with damped double integrator dynamics <sup>★</sup>

Mengxin Lyu <sup>a</sup>, Ruiliang Deng <sup>a</sup>, Zongying Shi <sup>a</sup>, Yisheng Zhong <sup>a</sup>

<sup>a</sup>*Department of Automation, Tsinghua University, Beijing 100084*

---

## Abstract

This paper studies a reach-avoid game of two damped double integrator players. An attacker aims to reach a static target, while a faster defender tries to protect the target by intercepting the attacker before it reaches the target. In scenarios where the defender succeeds, the defender aims to maximize the attacker's final distance from the target, while the attacker aims to minimize it. This work focuses on determining the equilibrium strategy in the defender-winning scenarios. The optimal state feedback strategy is obtained by a differential game approach combining geometric analysis. We construct a multiple reachable region to analyse the damped double integrator player's motion under optimal strategy. Building on this, a new type of the attacker's dominance region is introduced for the first time. It is shown that different strategies are required when the terminal point lies in distinct areas of the attacker's dominance region. Then, a necessary condition is derived for the proposed strategy to be optimal using differential game approach. Furthermore, a case where both players start at rest is discussed, and some useful properties about the dominance region and the optimal strategy are presented. Simulations are conducted to show the effectiveness of the proposed strategy.

---

## 1 Introduction

Differential game is an important topic with extensive applications such as robot navigation and collision avoidance [1], aerospace defense system [2], and region surveillance [3]. One specific type of differential game is the reach-avoid game, in which intelligent agents are divided into defenders and attackers. The defenders aim to protect a target region from the attackers, while the attackers attempt to reach the target before being intercepted by the defenders.

Reach-avoid differential game is first introduced and analyzed in [4] to derive equilibrium strategies. For players with simple motion, geometric method can be employed to provide intuitive solutions. Apollonius circles are used to represent regions that a player can reach before another player [5], i.e. dominance regions. For defenders with a non-zero capture radius, Cartesian ovals are used instead of Apollonius circles to represent dominance regions [6]. The target can take various forms, such as con-

vex shapes in a 2-D plane [7], a half-plane or hemisphere in the 3-D space [8,9], and obstructive target [10–12]. In active defense game [13–16], the target is also considered as a player with mobility, and the problem is formulated and solved as a three-player zero-sum differential game. Other studies focus on perimeter defense game, where defenders are restricted to moving along the boundary of the target region [17–19]. In these cases, geometric and differential game approaches are utilized to derive optimal strategies for defenders and attackers with simple motion. Scenarios involving multiple defenders or attackers have also been explored. In [20], two defenders try to intercept one attacker before it reaches the target region. The dominance regions of defenders and attacker are investigated to solve the game of kind and provide insights for the design of optimal strategies. In [21], a coastline protecting game with two attackers and one faster defender is studied by differential game approach, considering the existence of the singular surfaces. Deng et al. [22] further prove the optimal strategy and present a detailed discussion on the singular surfaces, utilizing geometric method and viscosity solution method to construct the value function. In more general multiplayer games, the problem can be decomposed into several sub-problems, each involving one attacker, and solved using matching algorithms [23–26].

While a simple motion model is convenient for geometric analysis to obtain analytical results, it often fails to accu-

---

<sup>★</sup> This work is supported in part by the National Natural Science Foundation of China under Grant U24B20173. (Corresponding author: Zongying Shi.)

*Email addresses:* lvmx23@mails.tsinghua.edu.cn (Mengxin Lyu), drl120@mails.tsinghua.edu.cn (Ruiliang Deng), szy@mail.tsinghua.edu.cn (Zongying Shi), zys-dau@mail.tsinghua.edu.cn (Yisheng Zhong).

rately represent real-world scenarios, where player's dynamics are more complex, and factors such as turning radius and damping need to be considered. Some research focuses on scenarios with Dubins cars and differential drive robots [27–30], considering minimum turning radius. Reference [31] studies a reach-avoid game of players with double integrator dynamics, provides conditions of capture in a single defender-attacker scenario, and address multiplayer case by a matching-based method. Wei et al. [32] investigate the dominance regions for the attacker and defender respectively in an active defense game with double integrator dynamics model, and design strategies grounded on the dominance regions. [33] addresses the active defense game with first order missile models, providing the optimal strategy for the target. A more realistic dynamic model is damped double integrator where the speed is constrained by a damping factor. Li et al. [34] derive strategies for a pursuit-evasion game with damped double integrator dynamics, using Hamilton-Jacobi-Isaacs (HJI) equations to prove the strategies' optimality. While games with more complex models have attracted attention, reach-avoid games of damped double integrator dynamics have not been considered in existing literature, and the properties of a damped double integrator player's motion under optimal strategy derived by differential game theory remain to be studied.

In this paper, a reach-avoid game involving one defender and one attacker with damped double integrator dynamics is considered. The optimal state feedback strategy is investigated by the Maximum Principle combining geometry method. Isochrones are utilized to analyze the players' reaching time and construct the attacker's dominance region (ADR) accordingly. Strategies for the attacker to reach different parts of the attacker's dominance region are then proposed, and a necessary condition for the strategies to be optimal is provided. The main contributions are as follow.

- (1) The motion of damped double integrator players under optimal strategy is studied, including the isochrones and the reaching times. We construct the multiple reachable region (MRR) analytically for each player based on the reaching times. What's more, the circumscribing and inscribing times of the attacker's and defender's isochrones are investigated. There are at most three and at least one circumscribing (or inscribing) times. A numerical method is proposed to identify all possible times.
- (2) The attacker's dominance region is constructed for the game, which is composed of multiple parts based on the relationship between the defender's and attacker's reaching times at a certain point. A new type of attacker's dominance region is introduced. The optimal strategy for the game is investigated building on the properties of ADR and MRR.
- (3) A necessary condition on the attacker's and de-

fender's reaching times for the proposed strategy to be optimal is derived using differential game approach. Furthermore, the optimal strategy for players initially at rest is derived.

The rest of this paper is organized as follows. We introduce the reach-avoid game of two damped double integrator players in Section 2, including problem formulation and notation. Section 3 first investigates the features of the optimal strategy. Then, an analysis of a single player's reaching time is carried out and the multiple reachable region is introduced. Based on that, we use the attacker's dominance region to determine the optimal strategy, along with the necessary condition for the proposed strategy to be optimal. Additionally, the special properties of the optimal strategy when both attacker and defender start at rest are provided. In Section 4, simulation results are given to demonstrate the performance of the proposed strategy in various situations. Finally, Section 5 concludes the article.

## 2 Problem Formulation

The problem considered in this paper is a reach-avoid game of one attacker (A) and one defender (D) both with damped double integrator dynamics. The attacker tries to reach the target at  $[0, 0]^T$  without being captured, while the defender aims to capture the attacker at the point as far as possible from the target.

The states of the attacker and defender are given by their Cartesian coordinates  $\mathbf{x}_A = [x_A, y_A]^T$ ,  $\mathbf{x}_D = [x_D, y_D]^T$  and velocity  $\mathbf{v}_A = [v_A, v_A]^T$ ,  $\mathbf{v}_D = [v_D, v_D]^T$ . The dynamics are described as follow:

$$\begin{cases} \dot{x}_i = v_{ix}, \\ \dot{y}_i = v_{iy}, \\ \dot{v}_{ix} = -\mu v_{ix} + u_i \cos \theta_i, \\ \dot{v}_{iy} = -\mu v_{iy} + u_i \sin \theta_i, \end{cases} \quad (1)$$

where  $u_i, \theta_i$  are the control inputs of player  $i$ ,  $i \in \{A, D\}$ .  $u_i$  represents the magnitude of acceleration, which is bounded, i.e.  $u_i \in [0, u_{im}]$ .  $\theta_i \in [0, 2\pi)$  is the direction of acceleration.  $\mu > 0$  denotes the damping factor, which is identical for the attacker and defender. We assume that the maximal acceleration of the attacker is smaller than that of the defender, i.e.  $\alpha = \frac{u_{Am}}{u_{Dm}} < 1$ . The game is illustrated in Fig. 1.

The terminal time is denoted as  $t_f$ , the terminal position of player  $i$  is denoted as  $\mathbf{x}_{if} = [x_{if}, y_{if}]^T = [x_i(t_f), y_i(t_f)]^T$  and the terminal velocity is  $\mathbf{v}_{if} = [v_{ixf}, v_{iyf}]^T = [v_{ix}(t_f), v_{iy}(t_f)]^T$ . Similarly, the initial position is  $\mathbf{x}_{i0} = [x_{i0}, y_{i0}]^T = [x_i(0), y_i(0)]^T$ , and the velocity is  $\mathbf{v}_{i0} = [v_{ix0}, v_{iy0}]^T = [v_{ix}(0), v_{iy}(0)]^T$ . In the defender-winning scenarios, the game terminates when

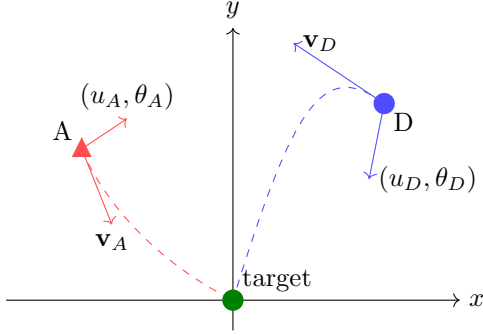


Fig. 1. An illustration of the reach-avoid game. The velocities of the attacker and defender are  $\mathbf{v}_A$  and  $\mathbf{v}_D$ . The control inputs are the accelerations  $(u_A, \theta_A)$  and  $(u_D, \theta_D)$ . The dashed lines are the trajectories of the attacker and defender.

the attacker is captured by the defender before reaching the target. The terminal equality constraint is

$$g(\mathbf{x}_{Af}, \mathbf{x}_{Df}) = \sqrt{(x_{Af} - x_{Df})^2 + (y_{Af} - y_{Df})^2} = 0. \quad (2)$$

And the terminal payoff function of the game is defined as

$$J(u_A, \theta_A, u_D, \theta_D; \mathbf{x}_{A0}, \mathbf{v}_{A0}, \mathbf{x}_{D0}, \mathbf{v}_{D0}) = \Phi(\mathbf{x}_{Af}), \quad (3)$$

where

$$\Phi(\mathbf{x}_{Af}) := \sqrt{x_{Af}^2 + y_{Af}^2}, \quad (4)$$

and we omit the dependence of  $u_i$  and  $\theta_i$  on  $t$  for brevity.

A complete information game is considered, i.e. the defender and attacker are assumed to be aware of the current states of both players. Due to that, the strategies of each player are mappings from the current states to the player's feasible control inputs. Denote the strategies as  $u_i(\mathbf{x}_A, \mathbf{x}_D, \mathbf{v}_A, \mathbf{v}_D)$ ,  $\theta_i(\mathbf{x}_A, \mathbf{x}_D, \mathbf{v}_A, \mathbf{v}_D)$ . The aim of this paper is to find the optimal strategies  $u_i^*$ ,  $\theta_i^*$  in the sense of Nash equilibrium; that is,

$$J(u_A^*, \theta_A^*, u_D, \theta_D) \leq J^* \leq J(u_A, \theta_A, u_D^*, \theta_D^*), \quad (5)$$

where  $J^* = J(u_A^*, \theta_A^*, u_D^*, \theta_D^*)$ ,

for all possible strategies  $u_i$ ,  $\theta_i$ . The value function of the game is given as the saddle point of the terminal payoff

$$V(\mathbf{x}_{A0}, \mathbf{v}_{A0}, \mathbf{x}_{D0}, \mathbf{v}_{D0}) = \min_{u_A, \theta_A} \max_{u_D, \theta_D} J, \quad (6)$$

subject to (1) and (2).

### 3 The Optimal Strategy in the Defender-Winning Scenarios

In this section, the optimal strategy of the reach-avoid game in the defender-winning scenarios is analysed.

Firstly, the properties of the optimal strategy are investigated using the Maximum Principle. Then, features of a single player's motion are studied by reaching times and multiple reachable region. Based on that, we construct the attacker's dominance region and show that the attacker must adopt distinct strategies to reach different parts of the region. Subsequently, a necessary condition for the proposed strategy to be optimal is derived. Finally, a case that both players are initially at rest is discussed.

#### 3.1 Hamiltonian and the Optimal Strategy

The Hamiltonian of differential game is given by

$$H = \lambda_1 v_{Dx} + \lambda_2 v_{Dy} + \gamma_1 v_{Ax} + \gamma_2 v_{Ay} + \lambda_3(-\mu v_{Dx} + u_D \cos \theta_D) + \lambda_4(-\mu v_{Dy} + u_D \sin \theta_D) + \gamma_3(-\mu v_{Ax} + u_A \cos \theta_A) + \gamma_4(-\mu v_{Ay} + u_A \sin \theta_A) \quad (7)$$

where  $\lambda = [\lambda_1, \lambda_2, \lambda_3, \lambda_4]^T$  is the co-state of the defender, and  $\gamma = [\gamma_1, \gamma_2, \gamma_3, \gamma_4]^T$  is the co-state of the attacker. The path equations for the defender's co-state are given by

$$\begin{aligned} [\dot{\lambda}_1, \dot{\lambda}_2]^T &= -\frac{\partial H}{\partial \mathbf{x}_D^T}, & [\dot{\lambda}_3, \dot{\lambda}_4]^T &= -\frac{\partial H}{\partial \mathbf{v}_D^T}, \\ [\lambda_{1f}, \lambda_{2f}]^T &= \frac{\partial \Phi}{\partial \mathbf{x}_{Df}^T} + \nu \frac{\partial g}{\partial \mathbf{x}_{Df}^T}, & (8) \\ [\lambda_{3f}, \lambda_{4f}]^T &= \frac{\partial \Phi}{\partial \mathbf{v}_{Df}^T} + \nu \frac{\partial g}{\partial \mathbf{v}_{Df}^T}, \end{aligned}$$

where  $\nu$  is a Lagrange multiplier. It can be obtained that

$$\begin{aligned} \dot{\lambda}_1 &= \dot{\lambda}_2 = 0, & \dot{\lambda}_3 &= -\lambda_1 + \mu \lambda_3, & \dot{\lambda}_4 &= -\lambda_2 + \mu \lambda_4, \\ \lambda_{3f} &= \lambda_{4f} = 0, \\ \lambda_{1f} &= \nu \frac{x_{Df} - x_{Af}}{\sqrt{(x_{Af} - x_{Df})^2 + (y_{Af} - y_{Df})^2}}, & (9) \\ \lambda_{2f} &= \nu \frac{y_{Df} - y_{Af}}{\sqrt{(x_{Af} - x_{Df})^2 + (y_{Af} - y_{Df})^2}}. \end{aligned}$$

The equations of  $\gamma$  are derived similarly. By solving co-states' path equations, one can obtain that

$$\begin{aligned} \lambda_1 &= \nu \frac{x_{Df} - x_{Af}}{\sqrt{(x_{Af} - x_{Df})^2 + (y_{Af} - y_{Df})^2}}, \\ \lambda_2 &= \nu \frac{y_{Df} - y_{Af}}{\sqrt{(x_{Af} - x_{Df})^2 + (y_{Af} - y_{Df})^2}}, \\ \lambda_3 &= \frac{\lambda_1}{\mu} (1 - e^{-\mu(t_f - t)}), & \lambda_4 &= \frac{\lambda_2}{\mu} (1 - e^{-\mu(t_f - t)}), \end{aligned} \quad (10)$$

$$\begin{aligned}
\gamma_1 &= \frac{x_{Af}}{\sqrt{x_{Af}^2 + y_{Af}^2}} + \nu \frac{x_{Af} - x_{Df}}{\sqrt{(x_{Af} - x_{Df})^2 + (y_{Af} - y_{Df})^2}}, \\
\gamma_2 &= \frac{y_{Af}}{\sqrt{x_{Af}^2 + y_{Af}^2}} + \nu \frac{y_{Af} - y_{Df}}{\sqrt{(x_{Af} - x_{Df})^2 + (y_{Af} - y_{Df})^2}}, \\
\gamma_3 &= \frac{\gamma_1}{\mu} (1 - e^{-\mu(t_f - t)}), \quad \gamma_4 = \frac{\gamma_2}{\mu} (1 - e^{-\mu(t_f - t)}).
\end{aligned} \tag{11}$$

The optimal strategies of the attacker and defender minimize and maximize the payoff function (4), respectively. According to Pontryagin Maximum Principle, we obtain the optimal strategy  $u_i^*$ ,  $\theta_i^*$  for the defender and attacker as

$$\begin{aligned}
u_A^* &= u_{Am}, \quad u_D^* = u_{Dm}, \\
\cos \theta_A^* &= -\frac{\gamma_3}{\sqrt{\gamma_3^2 + \gamma_4^2}}, \quad \sin \theta_A^* = -\frac{\gamma_4}{\sqrt{\gamma_3^2 + \gamma_4^2}}, \\
\cos \theta_D^* &= \frac{\lambda_3}{\sqrt{\lambda_3^2 + \lambda_4^2}}, \quad \sin \theta_D^* = \frac{\lambda_4}{\sqrt{\lambda_3^2 + \lambda_4^2}}.
\end{aligned} \tag{12}$$

By combining (10), (11) and (12), we know that both  $\theta_A^*$  and  $\theta_D^*$  are constant. Unless otherwise specified, in the following parts, a player's strategy is assumed to refer to a control input with  $u_i = u_{im}$  and a constant  $\theta_i$ ,  $i \in \{A, D\}$ . Then, based on (1) and (12), the trajectories of the attacker and defender are given by

$$\begin{aligned}
v_{ix}(t) &= v_{ix0}e^{-\mu t} + \frac{u_i \cos \theta_i}{\mu} (1 - e^{-\mu t}), \\
v_{iy}(t) &= v_{iy0}e^{-\mu t} + \frac{u_i \sin \theta_i}{\mu} (1 - e^{-\mu t}), \\
x_i(t) &= x_{i0} + \frac{v_{ix0}}{\mu} (1 - e^{-\mu t}) + \frac{u_i \cos \theta_i}{\mu} \left(t - \frac{1 - e^{-\mu t}}{\mu}\right), \\
y_i(t) &= y_{i0} + \frac{v_{iy0}}{\mu} (1 - e^{-\mu t}) + \frac{u_i \sin \theta_i}{\mu} \left(t - \frac{1 - e^{-\mu t}}{\mu}\right).
\end{aligned} \tag{13}$$

Therefore, the magnitude of velocity satisfies

$$\|\mathbf{v}_i\|_2 \leq \|\mathbf{v}_{i0}\|_2 e^{-\mu t} + \frac{u_{im}}{\mu} (1 - e^{-\mu t}) \xrightarrow{t \rightarrow \infty} \frac{u_{im}}{\mu}.$$

The initial velocity is assumed to satisfy  $\|\mathbf{v}_{i0}\|_2 \leq \frac{u_{im}}{\mu}$ .

As point capture is considered, the terminal positions for the attacker and defender should be the same, denoted as  $\mathbf{x}_f = \mathbf{x}_{Af} = \mathbf{x}_{Df}$ . According to (13), the optimal state feedback strategy  $\theta_i^*$ ,  $i \in \{A, D\}$  is given by

$$\begin{aligned}
\cos \theta_i^* &= \frac{x_f - x_{i0} - \frac{v_{ix0}}{\mu} (1 - e^{-\mu t_f})}{\frac{u_i}{\mu} (t_f - \frac{1 - e^{-\mu t_f}}{\mu})}, \\
\sin \theta_i^* &= \frac{y_f - y_{i0} - \frac{v_{iy0}}{\mu} (1 - e^{-\mu t_f})}{\frac{u_i}{\mu} (t_f - \frac{1 - e^{-\mu t_f}}{\mu})}.
\end{aligned} \tag{14}$$

The terminal time can be calculated through (13) once the terminal position is given.

### 3.2 Multiple Reachable Region

In this subsection, the isochrones of a player are analysed. Multiple reachable region is defined based on the player's reaching times to a certain point. The properties of the region's boundary are analyzed comprehensively to underlie the subsequent construction of the dominance region and the analysis of the optimal terminal position.

The isochron at  $t$  of player  $i$ ,  $i \in \{A, D\}$  refers to the set of possible positions of player  $i$  at  $t$  under constant  $\theta_i$  and  $u_{im}$ . As derived in [34], the isochron  $\mathcal{I}_i(t)$  is a circle with radius  $r_{ic}(t)$  and center  $\mathbf{x}_{ic}(t) = [x_{ic}(t), y_{ic}(t)]^T$  given by

$$\begin{aligned}
r_{ic}(t) &= \frac{u_{im}}{\mu} \left(t - \frac{1 - e^{-\mu t}}{\mu}\right), \\
x_{ic}(t) &= x_{i0} + \frac{v_{ix0}}{\mu} (1 - e^{-\mu t}), \\
y_{ic}(t) &= y_{i0} + \frac{v_{iy0}}{\mu} (1 - e^{-\mu t}).
\end{aligned} \tag{15}$$

**Lemma 1.** Given  $\mathbf{x}_{i0}$  and  $\mathbf{v}_{i0}$ ,  $\{\mathbf{x} \in \mathbb{R}^2 \mid \|\mathbf{x} - \mathbf{x}_{ic}(t)\|_2 \leq r_{ic}(t)\}$  is the set of points that player  $i$  can reach at  $t$ .

The proof is given in Appendix A.

Define functions about the radius of isochrones and the distance between  $\mathbf{x}_{Ac}$  and  $\mathbf{x}_{Dc}$

$$\begin{aligned}
\Gamma_{in}(t) &= \|\mathbf{x}_{Ac} - \mathbf{x}_{Dc}\|_2^2 - (r_{Ac} - r_{Dc})^2 = o(t) - p_{in}(t), \\
\Gamma_{out}(t) &= \|\mathbf{x}_{Ac} - \mathbf{x}_{Dc}\|_2^2 - (r_{Ac} + r_{Dc})^2 = o(t) - p_{out}(t), \\
o(t) &= \|\Delta \mathbf{x}\|_2^2 + \frac{\|\Delta \mathbf{v}\|_2^2}{\mu^2} (1 - e^{-\mu t})^2 \\
&\quad + 2 \frac{1}{\mu} \Delta \mathbf{x}^T \Delta \mathbf{v} (1 - e^{-\mu t}), \\
p_{in}(t) &= \frac{(u_A - u_D)^2}{\mu^2} \left(t - \frac{1 - e^{-\mu t}}{\mu}\right)^2, \\
p_{out}(t) &= \frac{(u_A + u_D)^2}{\mu^2} \left(t - \frac{1 - e^{-\mu t}}{\mu}\right)^2,
\end{aligned} \tag{16}$$

where  $\Delta \mathbf{x} = \mathbf{x}_{A0} - \mathbf{x}_{D0}$ ,  $\Delta \mathbf{v} = \mathbf{v}_{A0} - \mathbf{v}_{D0}$ . Obviously, the isochrones  $\mathcal{I}_A(t)$  and  $\mathcal{I}_D(t)$  inscribe if function  $\Gamma_{in}(t) = 0$ , circumscribe if  $\Gamma_{out}(t) = 0$ .

**Theorem 1.**  $\mathcal{I}_A(t)$  and  $\mathcal{I}_D(t)$  inscribe (circumscribe) for at least one time and at most three times.

The proof is given in Appendix B.

**Corollary 1.** For any static point  $\mathbf{x} \in \mathbb{R}^2$ , a player has at most three and at least one strategy to reach  $\mathbf{x}$ .

*Proof.* Let  $u_A = 0$ ,  $\mathbf{v}_{A0} = [0, 0]^T$  and  $\mathbf{x}_{A0} = \mathbf{x}$ , then  $\mathcal{I}_D(t)$  passing  $\mathbf{x}$  is equivalent to  $\mathcal{I}_D(t)$  and  $\mathcal{I}_A(t)$  circumscribing. Therefore, according to Theorem 1,  $\mathcal{I}_D(t)$  passes  $\mathbf{x}$  for at least one time and at most three times. So the defender has at least one strategy and at most three strategies to reach a given position  $\mathbf{x}$ . Analogously, the attacker has at least one and at most three strategies to reach  $\mathbf{x}$ .  $\square$

Now, we introduce the concept of multiple reachable region and analyse its properties for later proofs.

**Definition 1** (Multiple Reachable Region). Given  $\mathbf{x}_{i0}$  and  $\mathbf{v}_{i0}$ , the multiple reachable region of player  $i$ , designated by  $\mathcal{M}_i$ ,  $i \in \{A, D\}$ , is the set of points in  $\mathbb{R}^2$  that player  $i$  has multiple strategies to reach.

An illustration of  $\mathcal{M}_i$  is shown in Fig. 2(a), where the elements will be introduced in the subsequent discussion. There should exist three distinct times for the player to reach a certain point in  $\mathcal{M}_i$ .

**Definition 2** (Reaching Time). Given initial state  $\mathbf{x}_{A0}$  and  $\mathbf{v}_{A0}$ , the time for the attacker to arrive at  $\mathbf{x}$  is denoted as the reaching time  $t_{Aj}(\mathbf{x}, \mathbf{x}_{A0}, \mathbf{v}_{A0})$ , where  $j \in \{1, 2, 3\}$  for  $\mathbf{x} \in \mathcal{M}_A$  and  $j = 0$  for  $\mathbf{x} \in \mathbb{R}^2 \setminus \mathcal{M}_A$ . The reaching time outside  $\mathcal{M}_A$  is abbreviated as  $t_A$  hereinafter.

Given  $\mathbf{x}_{D0}$  and  $\mathbf{v}_{D0}$ , the reaching time for the defender to a given point  $\mathbf{x}$  is  $t_{Dk}(\mathbf{x}, \mathbf{x}_{D0}, \mathbf{v}_{D0})$ , where  $k \in \{1, 2, 3\}$  for  $\mathbf{x} \in \mathcal{M}_D$  and  $k = 0$  for  $\mathbf{x} \in \mathbb{R}^2 \setminus \mathcal{M}_D$ . The reaching time outside  $\mathcal{M}_D$  is abbreviated as  $t_D$  hereinafter.

The order of magnitude of player  $i$ 's reaching times in  $\mathcal{M}_i$  is  $t_{i1}(\mathbf{x}) < t_{i2}(\mathbf{x}) < t_{i3}(\mathbf{x})$ .

The variables about the initial states are omitted without ambiguity.  $t_i(\mathbf{x})$ ,  $i \in \{A, D\}$  is continuous in  $\mathbb{R}^2 \setminus \mathcal{M}_i$ .  $t_{i1}(\mathbf{x}), t_{i2}(\mathbf{x}), t_{i3}(\mathbf{x})$  are continuous in  $\mathcal{M}_i$ . An illustration of reaching times to a position  $\mathbf{x}$  in  $\mathcal{M}_i$  and corresponding isochrones is given in Fig. 2(b).

The boundary of  $\mathcal{M}_i$ , denoted as  $\partial\mathcal{M}_i$ , is the set of points where the player has two strategies to reach, i.e. two of the three reaching times equal at  $\mathbf{x} \in \partial\mathcal{M}_i$ . The gradients of the two equal reaching times do not exist at  $\mathbf{x}$ ; otherwise, there will be more than one reaching time outside  $\mathcal{M}_i$ .

The gradients of reaching time  $t_{ij}(\mathbf{x})$ ,  $i \in \{A, D\}$ ,  $j \in \{1, 2, 3\}$  can be derived using (13) by taking the derivative of  $t$  and  $\theta$  with respect to  $\mathbf{x}$

$$\frac{dt_{ij}(\mathbf{x})}{d\mathbf{x}} = \frac{1}{v_{ix} \cos \theta_i + v_{iy} \sin \theta_i} [\cos \theta_i, \sin \theta_i]^T, \quad (17)$$

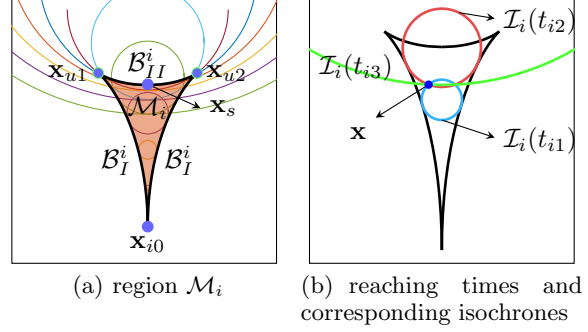


Fig. 2. An illustration of isochrones and region  $\mathcal{M}_i$  of a player. The isochrones are marked by colored circles, and the region  $\mathcal{M}_i$  is shaded in Fig 2(a). The player has three strategies to reach a point  $\mathbf{x} \in \mathcal{M}_i$ , with corresponding isochrones shown in Fig 2(b). For points outside  $\mathcal{M}_i$ , the player has one strategy to reach. On the boundary of the area, denoted as  $\mathcal{B}_I^i, \mathcal{B}_{II}^i$ , the player has two strategies.

where  $v_{ix}, v_{iy}$  are the velocity of player  $i$  when it reaches  $\mathbf{x}$  at  $t_{ij}(\mathbf{x})$ , and  $\theta_i$  is the corresponding strategy. From a geometric perspective, the points on  $\partial\mathcal{M}_i$  are the tangent points between the player's trajectories  $(\mathbf{x}_i(t))$  under the strategy with a constant  $\theta_i$  and  $u_i = u_{im}$  and the isochrones. This can be understood through the condition of tangency:

$$\frac{v_{iy}(t, \theta_i)}{v_{ix}(t, \theta_i)} = -\cot \theta_i,$$

which can be rewritten as

$$v_{iy0} \sin \theta_i + v_{ix0} \cos \theta_i + \frac{u_i}{\mu} (e^{\mu t} - 1) = 0. \quad (18)$$

Equation (18) is equivalent to the condition where the gradient given by (17) does not exist.

To construct the multiple reachable region analytically, it is necessary to derive the formulation of points on  $\partial\mathcal{M}_i$ . To this end, we introduce the concept of self-overlapping.

$\mathcal{I}_i(t)$  self-overlaps if  $\exists T$ , s.t.  $\forall \Delta t \in (0, T)$ ,  $\mathcal{I}_i(t)$  intersects with  $\mathcal{I}_i(t - \Delta t)$ . If  $\mathcal{I}_i(t)$  and  $\mathcal{I}_i(t - \Delta t)$  intersect, the intersections are symmetric with respect to  $\mathbf{v}_{i0}$ , denoted as the self-overlapping intersections  $\mathbf{x}_{int}^{\pm}(\Delta t, t)$ , where  $(\mathbf{x}_{int}^+(\Delta t, t) - \mathbf{x}_{i0}) \wedge \mathbf{v}_{i0} \geq 0$  and  $(\mathbf{x}_{int}^-(\Delta t, t) - \mathbf{x}_{i0}) \wedge \mathbf{v}_{i0} \leq 0$  ( $\wedge$  is the wedge product of two vectors).

**Remark 1.** When  $\Delta t = 0$ , the two isochrones are identical, so the self-overlapping intersections do not exist at  $\Delta t = 0$ . However, the self-overlapping intersections exist when  $\Delta t \rightarrow 0$ , which will be shown later. Therefore, we define that  $\Delta t > 0$  for  $\mathbf{x}_{int}^{\pm}(\Delta t, t)$  and  $\lim_{\Delta t \rightarrow 0} \mathbf{x}_{int}^{\pm}(\Delta t, t)$  exists.

Next, we associate the existence of tangent points with self-overlapping.

**Lemma 2.** If  $\mathcal{I}_i$  self-overlaps at  $t$ , there exist two trajectories of player  $i$  tangent to  $\mathcal{I}_i(t)$ . The tangent points are  $\lim_{\Delta t \rightarrow 0} \mathbf{x}_{int}^{\pm}(\Delta t, t)$ .

*Proof.* Without loss of generality, assume  $v_{iy0} = 0$ ,  $\mathbf{x}_{i0} = [0, 0]^T$ . For brevity,  $\lim_{\Delta t \rightarrow 0} \mathbf{x}_{int}^{\pm}(\Delta t, t)$  are denoted as  $\mathbf{x}_{int}^{\pm}(t)$  in the following part. We first work out the expression of  $\mathbf{x}_{int}^{\pm}(t)$ . Keep only the first-order of  $\Delta t$

$$e^{-\mu(t-\Delta t)} \approx e^{-\mu t} + \mu e^{-\mu t} \Delta t.$$

The  $x$ -coordinate of the center of isochron  $x_{ic}(t - \Delta t)$  and the radius  $r_{ic}(t - \Delta t)$  defined in (15) can be approximated as:

$$\begin{aligned} r_{ic}(t - \Delta t) &= \frac{u_i}{\mu} \left( t - \Delta t - \frac{1 - e^{-\mu t} - \Delta t \mu e^{-\mu t}}{\mu} \right) \\ &= \frac{u_i}{\mu} \left( t - \frac{1 - e^{-\mu t}}{\mu} - \Delta t(1 - e^{-\mu t}) \right), \\ x_{ic}(t - \Delta t) &= \frac{v_{ix0}}{\mu} (1 - e^{-\mu t}) - \Delta t v_{ix0} e^{-\mu t}. \end{aligned} \quad (19)$$

The  $y$ -coordinate of the center of isochron  $y_{ic}(t - \Delta t) = 0$  because the initial velocity  $v_{iy0} = 0$ . The equations of the two intersecting isochrones are

$$\begin{aligned} (x - x_{ic}(t))^2 + y^2 &= r_{ic}^2(t), \\ (x - x_{ic}(t - \Delta t))^2 + y^2 &= r_{ic}^2(t - \Delta t), \end{aligned} \quad (20)$$

from which it follows that

$$-2(x - x_{ic}(t)) \Delta t v_{ix0} e^{-\mu t} = 2r_{ic}(t) \frac{u_i}{\mu} \Delta t (1 - e^{-\mu t}) + o(\Delta t), \quad (21)$$

and by taking the limit as  $t$  approaches 0, we obtain

$$-(x - x_{ic}(t)) v_{ix0} e^{-\mu t} = r_{ic}(t) \frac{u_i}{\mu} (1 - e^{-\mu t}). \quad (22)$$

Thus the  $x$ -coordinates of the intersection points can be written as

$$x_{int}^{\pm}(t) - x_{ic}(t) = -r_{ic}(t) \frac{u_i}{\mu} \frac{1 - e^{-\mu t}}{v_{ix0} e^{-\mu t}}. \quad (23)$$

The corresponding strategy can be computed using the relationship between the intersections and isochron's center:

$$\cos \theta_i = \frac{x_{int}^{\pm}(t) - x_{ic}(t)}{r_{ic}(t)} = -\frac{u_i}{\mu} \frac{1 - e^{-\mu t}}{v_{ix0} e^{-\mu t}}. \quad (24)$$

By substituting (24) into (18), it can be verified that the trajectories are tangent to  $\mathcal{I}_i$  at the intersections.  $\square$

The moment after which player's isochrones do not self-overlap anymore is called barrier time [34], which can be expressed as

$$t_{is} = \frac{1}{\mu} \ln \frac{\mu \sqrt{v_{ix0}^2 + v_{iy0}^2} + u_{im}}{u_{im}}, \quad i \in \{A, D\}. \quad (25)$$

According to Lemma 2,  $\partial \mathcal{M}_i$  can be constructed by  $\lim_{\Delta t \rightarrow 0} \mathbf{x}_{int}^{\pm}(\Delta t, t)$  before the barrier time. At  $t_{is}$ , it can be derived from (24) that  $\cos \theta_i = -1$  if  $v_{iy0} = 0$ . So, there is only one solution for  $\lim_{\Delta t \rightarrow 0} \mathbf{x}_{int}^{\pm}(\Delta t, t_{is})$ , denoted as  $\mathbf{x}_s$ . We should note here that  $\mathbf{x}_s$  belongs to player  $i$  although it does not have a subscript  $i$ . This is because the notation is only used in this section to investigate  $\mathcal{M}_i$  and will not cause confusion in places where the attacker and defender are both involved.

There are only two possible combinations of equal reaching times:  $t_{i1}(\mathbf{x}) = t_{i2}(\mathbf{x})$  and  $t_{i2}(\mathbf{x}) = t_{i3}(\mathbf{x})$ . Depending on which two reaching times equal to each other,  $\partial \mathcal{M}_i$  can be categorized into two types of curves  $\mathcal{B}_I^i$  and  $\mathcal{B}_{II}^i$  given by

$$\begin{aligned} \mathcal{B}_I^i &= \{\mathbf{x} \in \mathbb{R}^2 | t_{i1}(\mathbf{x}) = t_{i2}(\mathbf{x})\}, \\ \mathcal{B}_{II}^i &= \{\mathbf{x} \in \mathbb{R}^2 | t_{i2}(\mathbf{x}) = t_{i3}(\mathbf{x})\}. \end{aligned} \quad (26)$$

It can be observed from Fig. 2(a) that the boundary is not smooth at two symmetric cusps  $\mathbf{x}_{u1}$  and  $\mathbf{x}_{u2}$ , where the tangent vector of the boundary does not exist. Next, we investigate the time when the player's isochrones pass  $\mathbf{x}_{u1}$ , which is essential for constructing  $\mathcal{M}_i$  using self-overlapping intersections. Denote  $\mathbf{x}(t)$  as the point on  $\partial \mathcal{M}_i$  with the parameter  $t$  referring to the two equal reaching times. The tangent vector of  $\partial \mathcal{M}_i$  at  $\mathbf{x}(t)$  can be derived based on (13):

$$\frac{d\mathbf{x}}{dt} = \mathbf{v}_i(t, \theta_i) + \frac{u_i}{\mu} \left( t - \frac{1 - e^{-\mu t}}{\mu} \right) \frac{d\theta_i}{dt} [-\sin \theta_i, \cos \theta_i]^T, \quad (27)$$

where  $\theta_i$  is derived from the tangential condition (18):

$$\begin{aligned} \sin \theta_i &= \frac{-v_{iy0} \frac{u_i}{\mu} (e^{\mu t} - 1) \pm v_{ix0} M}{v_{ix0}^2 + v_{iy0}^2}, \\ \cos \theta_i &= -\frac{v_{ix0} \frac{u_i}{\mu} (e^{\mu t} - 1) \pm v_{iy0} M}{v_{ix0}^2 + v_{iy0}^2}, \end{aligned} \quad (28)$$

here  $M = \sqrt{v_{ix0}^2 + v_{iy0}^2 - \frac{u_i^2}{\mu^2} (e^{\mu t} - 1)^2}$ . We get  $\frac{d\theta_i}{dt}$  as

$$\frac{d\theta_i}{dt} = \frac{1}{\cos \theta_i} \frac{d \sin \theta_i}{dt} = \pm \frac{e^{\mu t} u_i}{M}. \quad (29)$$

According to (18),  $\mathbf{v}_i(t, \theta_i)$  is parallel to  $[-\sin \theta_i, \cos \theta_i]^T$ . Therefore, the tangent vector is initially in the same

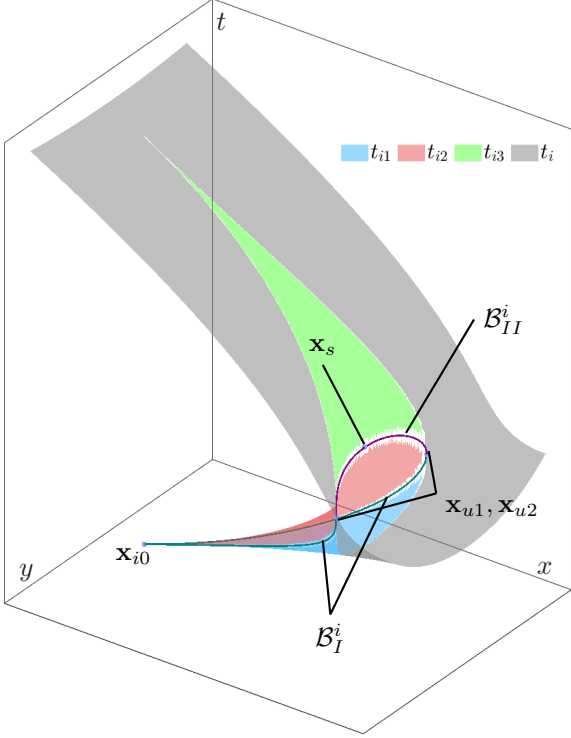


Fig. 3. An illustration of the reaching times of player  $i$ .

direction with  $\mathbf{v}_i(t, \theta_i)$ , then equals to  $\mathbf{0}$  at  $\mathbf{x}_{u1}$  and  $\mathbf{x}_{u2}$ . After that, it is in the opposite direction with the velocity. The time  $t_u := t_{i2}(\mathbf{x}_{u1}) = t_{i2}(\mathbf{x}_{u2})$  is determined by solving  $\frac{d\mathbf{x}}{dt} = \mathbf{0}$ :

$$\frac{u_i}{\mu} \left( t_u - \frac{1 - e^{-\mu t_u}}{\mu} \right) \frac{e^{\mu t_u} u_i}{M} = \|\mathbf{v}_i(t_u, \theta_i)\|_2, \quad (30)$$

$$= M e^{-\mu t_u}.$$

Hence,  $t_u$  satisfies the following equation:

$$\frac{u_i^2}{\mu} \left( t_u - \frac{1 - e^{-\mu t_u}}{\mu} \right) = \|\mathbf{v}_{i0}\|_2^2 e^{-2\mu t_u} - \frac{u_i^2}{\mu^2} (1 - e^{-\mu t_u})^2. \quad (31)$$

Period  $[0, t_{is}]$  can be divided into two phases:  $[0, t_u]$  and  $[t_u, t_{is}]$ . The initial position  $\mathbf{x}_{i0} \in \mathcal{B}_I^i$ , because  $t_{i1}(\mathbf{x}_{i0}) = t_{i2}(\mathbf{x}_{i0}) = 0$ , and  $t_{i3}(\mathbf{x}_{i0}) > 0$  if  $\|\mathbf{v}_{i0}\|_2 > 0$ . As for  $\mathbf{x}_s$ , since  $\lim_{\Delta t \rightarrow 0} \mathbf{x}_{int}^\pm(\Delta t, t_{is}) = \mathbf{x}_s$  and  $\mathcal{I}_i(t)$  do not pass  $\mathbf{x}_s$  after  $t_{is}$ ,  $t_{i2}(\mathbf{x}_s) = t_{i3}(\mathbf{x}_s)$ . Thus,  $\mathbf{x}_s$  is on  $\mathcal{B}_{II}^i$ . An illustration of the reaching times is given in Fig. 3. In the first phase,  $t_{i1} = t_{i2}$ . The intersections start from  $\mathbf{x}_{i0}$  and end at  $\mathbf{x}_{u1}$  and  $\mathbf{x}_{u2}$  as  $t_{i1}$  and  $t_{i2}$  increase, forming  $\mathcal{B}_I^i$ . In the second phase,  $t_{i2} = t_{i3}$ . The intersections start from  $\mathbf{x}_{u1}$  and  $\mathbf{x}_{u2}$  and end at  $\mathbf{x}_s$ , forming  $\mathcal{B}_{II}^i$ . On  $\mathcal{B}_I^i$ , as  $t_{i2}$  increases to  $t_u$ ,  $t_{i1}$  increases while  $t_{i3}$  decreases to  $t_u$ . On  $\mathcal{B}_{II}^i$ , as  $t_{i2}$  increases to  $t_{is}$ ,  $t_{i3}$  increases while  $t_{i1}$  decreases from  $t_u$ . At  $\mathbf{x}_{u1}$  and  $\mathbf{x}_{u2}$ ,  $t_{i1} = t_{i2} = t_{i3}$ . Therefore, for  $\mathbf{x} \in \mathcal{M}_i$ ,  $t_{i1}(\mathbf{x}) \leq t_u \leq t_{i3}(\mathbf{x})$ ,  $t_{i2}(\mathbf{x}) \leq t_{is}$ .

Moreover, the following statements about the continuity of reaching times hold:

$\mathbf{x} \in \mathcal{B}_I^i$ ,  $\forall \epsilon > 0, \exists \delta > 0$ , s.t.  $\forall \mathbf{x}' \in \mathbb{R}^2 \setminus \mathcal{M}_i$ , if  $\|\mathbf{x} - \mathbf{x}'\| < \delta$ , then  $|t_i(\mathbf{x}') - t_{i3}(\mathbf{x})| < \epsilon$ ,

$\mathbf{x} \in \mathcal{B}_{II}^i$ ,  $\forall \epsilon > 0, \exists \delta > 0$ , s.t.  $\mathbf{x}' \in \mathbb{R}^2 \setminus \mathcal{M}_i$ , if  $\|\mathbf{x} - \mathbf{x}'\| < \delta$ , then  $|t_i(\mathbf{x}') - t_{i1}(\mathbf{x})| < \epsilon$ .

(32)

Next, the reachability of a player to a certain point is analysed.

**Lemma 3.**  $\forall \mathbf{x} \in \mathcal{M}_i$  and  $\forall t \in (t_{i2}(\mathbf{x}), t_{i3}(\mathbf{x}))$ ,  $\mathbf{x}_i(t, \theta_i(t), u_i(t)) \neq \mathbf{x}$  for all  $\theta_i(t)$  and  $u_i(t)$ . That is, there exists a period that the player  $i$  cannot reach  $\mathbf{x}$  regardless of its strategy.

*Proof.* We can infer from the proof of Theorem 1 that for  $t \in (t_{i2}, t_{i3})$ ,  $\|\mathbf{x} - \mathbf{x}_{ic}(t)\|_2 > r_{ic}(t)$ . According to Lemma 1, the player can not reach  $\mathbf{x}$  at  $t$ .  $\square$

Similarly, for  $t \in (t_{i1}(\mathbf{x}), t_{i2}(\mathbf{x}))$ ,  $\mathbf{x}$  is contained within the isochrones, i.e. the player has strategies to reach  $\mathbf{x}$  during  $t_{i1}(\mathbf{x})$  and  $t_{i2}(\mathbf{x})$ .

### 3.3 Attacker's Dominance Region

As defined in [4], the attacker's dominance region (ADR) is the region where the attacker can reach without being captured. In this section, we first define the typical attacker's dominance region for this problem. Then, a new type of the attacker dominance region is introduced.

**Definition 3 (ADR).** The typical attacker's dominance region is the set of points where  $\exists j \in \{0, 1, 2, 3\}$  such that the attacker reaches at the point at  $t_{Aj}$  and it is outside  $\mathcal{I}_D(t_{Aj})$ .

$$\text{ADR} = \{ \mathbf{x} \in \mathbb{R}^2 \mid \|\mathbf{x} - \mathbf{x}_{Ac}(t_{Aj})\|_2 = r_{Ac}(t_{Aj}), \|\mathbf{x} - \mathbf{x}_{Dc}(t_{Aj})\|_2 > r_{Dc}(t_{Aj}) \}. \quad (33)$$

The attacker's dominance region is further divided into two types. The first type of ADR, denoted as  $\mathcal{R}_I$ , is given by:

$$\mathcal{R}_I = \{ \mathbf{x} \in \mathbb{R}^2 \mid \mathbf{x}_A(\theta_A^*, u_{Am}, t_{Aj}) = \mathbf{x}, \text{ and } \|\mathbf{x}_A(\theta_A^*, u_{Am}, t) - \mathbf{x}_{Dc}(t)\|_2 > r_{Dc}(t), \forall t < t_{Aj} \}, \quad (34)$$

where  $\theta_A^*$  is the strategy for the attacker to reach  $\mathbf{x}$  at  $t_{Aj}$ . That is, the attacker can reach the point with its maximum acceleration and a constant  $\theta_A$  without being captured.

The second type of ADR is  $\mathcal{R}_{II} = \text{ADR} \setminus \mathcal{R}_I$ , which means that there exists defender's strategy to capture the attacker with  $u_A = u_{Am}$  and a constant  $\theta_A^*$ .

**Remark 2.** If the players are with simple motion models, Definition 3 is the attacker's dominance region used in other works [20], hence it is defined as the typical attacker's dominance region. However, with damped double integrator players, only the first type of ADR is the region that the attacker can reach early than the defender and will not be captured. As the optimal trajectory of the player with damped double integrator dynamics in the reach-avoid game is not always a straight line, the attacker arriving earlier than the defender at point  $\mathbf{x}$  does not guarantee the attacker arriving earlier than the defender along the attacker's whole trajectory. Therefore, the second type of the attacker dominance region exists for the damped double integrator player.

It can be inferred from Lemma 3 that  $\mathcal{R}_I \cup \mathcal{R}_{II}$  is the set of points where exists  $j$  such that  $t_{Aj}(\mathbf{x}) < \min t_D(\mathbf{x})$  or  $t_{D2}(\mathbf{x}) < t_{Aj}(\mathbf{x}) < t_{D3}(\mathbf{x})$ . The notation  $\min t_D(\mathbf{x})$  refers to the minimum time for the defender to reach  $\mathbf{x}$ , i.e.  $\min t_D(\mathbf{x}) = t_{D1}$  if  $\mathbf{x} \in \mathcal{M}_D$ , and  $\min t_D(\mathbf{x}) = t_D$  if  $\mathbf{x} \in \mathbb{R}^2 \setminus \mathcal{M}_D$ . At the intersections of the attacker's and defender's isochrones, the reaching times of the attacker and defender equal, so the intersections form a part of the boundary of  $\mathcal{R}_I \cup \mathcal{R}_{II}$ , denoted as  $\mathcal{L}$ . Moreover, on two sides of  $\mathcal{B}_I^A$ , the relationship of the reaching times could be  $t_{A1} < t_D < t_{A3}$  and  $t_A > t_D$  respectively. Therefore,  $\mathcal{B}_I^A$  may also be a part of the attacker's dominance region's boundary. However, the attacker will not be captured on  $\mathcal{B}_I^A$  because the attacker's and defender's reaching times are not equal along  $\mathcal{B}_I^A$ . Therefore, the points on  $\mathcal{B}_I^A$  are not feasible terminal positions and will not be discussed in this paper.

To investigate the intersections of isochrones, the circumscribing and inscribing times of the attacker's and defender's isochrones are needed. Isochrones  $\mathcal{I}_A$  and  $\mathcal{I}_D$  first circumscribe at  $t_{out}$ , which represents the earliest time for the defender to capture the attacker. Before  $t_{out}$ , regardless of the strategy the defender adopts, it is unable to capture the attacker. The isochrones  $\mathcal{I}_A$  and  $\mathcal{I}_D$  first inscribe at  $t_{in}$  when the reachable region of the attacker is completely contained in the region of the defender, which represents the latest time of capture under the attacker's effort [34]. Hence, for the rest of the discussion, we only focus on the time interval  $[0, t_{in}]$  and assume that  $t < t_{in}$  throughout.

The isochrones circumscribe before they first inscribe because they are initially separated. After that, if isochrones circumscribe for another time, which means  $\mathcal{I}_A$  and  $\mathcal{I}_D$  are separated again, they will circumscribe subsequently for a third time, as the attacker's reachable region will eventually be contained in the defender's. Similarly, if the isochrones inscribe for a second time,

they will inscribe for one more time. As shown in Fig. 4, the isochrones in Fig. 4(a) circumscribe and inscribe for one time. The isochrones in Fig. 4(b) circumscribe and inscribe for three times, but only the period before the first inscribing time is considered. The boundary  $\mathcal{B}_I^A$  is also a part of the boundary of ADR in this example. In Fig. 4(c), the isochrones circumscribe for three times before they inscribe.

Three circumscribing times are all required to be accurately calculated to construct the boundary of the attacker's dominance region. However, since the function  $\Gamma_{in}$  and  $\Gamma_{out}$  may not be monotonous or may cross  $x = 0$  more than once, it is difficult to directly solve for the zero points of  $\Gamma_{in}(t)$  and  $\Gamma_{out}(t)$ . Especially in the situation shown in Fig. 4(b) where the attacker and defender are close initially so  $t_{out}$  and  $t_{in}$  are relatively small and thus easily overlooked. To address this problem, we utilize the properties analysed in the proof of Theorem 1 to derive Algorithm 1 to solve the circumscribing and inscribing times by dividing  $t > 0$  into parts with at most one zero point, which ensures that the search algorithm for zero point can be applied.

---

**Algorithm 1** Circumscribing and Inscribing Time Solver

---

```

1: Input:  $\Delta\mathbf{x}, \Delta\mathbf{v}, \mu, \Gamma$  % function  $\Gamma$  refers to  $\Gamma_{in}$ 
   or  $\Gamma_{out}$  given in (16)
2: Output:  $t$  % circumscribing or inscribing times
   % FindZeroPoint( $f(t), t_{left}, t_{right}$ ) is a function to
   find single zero point for  $f(t)$  in  $[t_{left}, t_{right}]$ 
3: if  $\Delta\mathbf{v}^2 + \mu\Delta\mathbf{x}^T\Delta\mathbf{v} < 0$  then
4:    $t \leftarrow \text{FindZeroPoint}(\Gamma, 0, +\infty)$ 
5: else if  $\Delta\mathbf{x}^T\Delta\mathbf{v} > 0$  then
6:    $t \leftarrow \text{FindZeroPoint}(\Gamma, 0, +\infty)$ 
7: else
8:   % there may exist more than one zero point
9:    $t_{d-max} \leftarrow \text{FindZeroPoint}(\Gamma', 0, +\infty)$ 
10:  if  $\Gamma''(t_{d-max}) < 0$  then
11:     $t \leftarrow \text{FindZeroPoint}(\Gamma, 0, +\infty)$ 
12:  else
13:     $t_{min} \leftarrow \text{FindZeroPoints}(\Gamma', 0, t_{d-max})$ 
14:     $t_{max} \leftarrow \text{FindZeroPoints}(\Gamma', t_{d-max}, +\infty)$ 
15:    if  $\Gamma(t_{min}) > 0$  then
16:       $t \leftarrow \text{FindZeroPoint}(\Gamma, t_{max}, +\infty)$ 
17:    else if  $\Gamma(t_{max}) < 0$  then
18:       $t \leftarrow \text{FindZeroPoint}(\Gamma, 0, t_{min})$ 
19:    else
20:       $t_1 \leftarrow \text{FindZeroPoints}(\Gamma, 0, t_{min})$ 
21:       $t_2 \leftarrow \text{FindZeroPoints}(\Gamma, t_{min}, t_{max})$ 
22:       $t_3 \leftarrow \text{FindZeroPoints}(\Gamma, t_{max}, +\infty)$ 
23:       $t \leftarrow [t_1, t_2, t_3]$ 
24:    end if
25:  end if
26: end if
27: return  $t$ 

```

---

Apart from  $\mathcal{R}_I$  and  $\mathcal{R}_{II}$ , from Lemma 3, we can find out that if the attacker can reach a point  $\mathbf{x} \in \mathcal{M}_D$  before

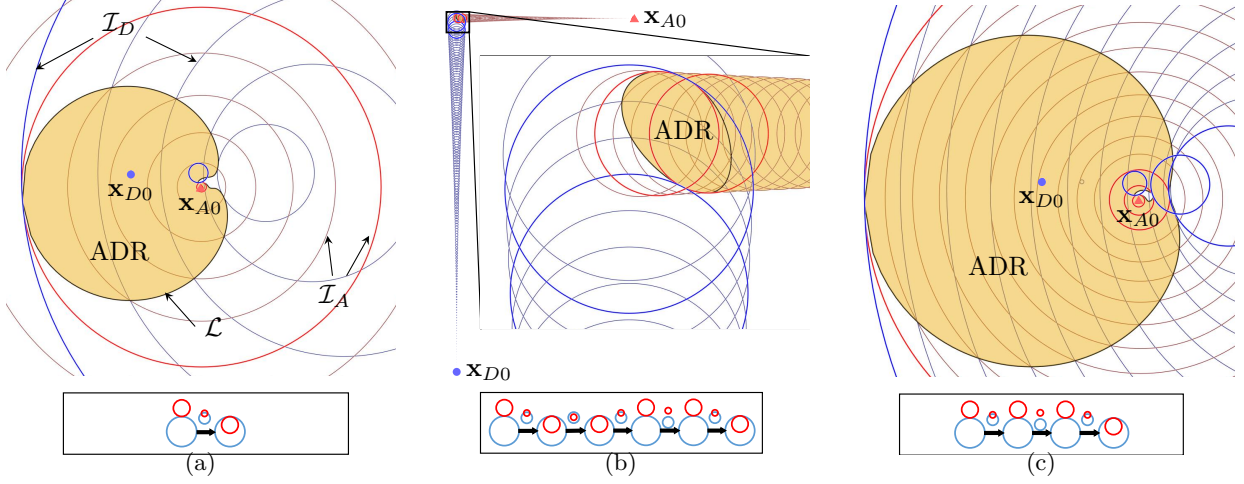


Fig. 4. Illustrations of dominance regions. The yellow shaded regions indicate the attacker's dominance regions (ADR). Blue and red circles represent isochrones of the defender and attacker, and inscribe circle and circumscribe circles are displayed in bold. The intersections of isochrones form the black curve  $\mathcal{L}$ . Boxes at the bottom of each figure are schematics of the tangential orders, with intermediate states above the arrows. The red and blue circles in schematics represent attacker's and defender's isochrones. Three different tangential orders are given.

$t_{D3}(\mathbf{x})$ , it is possible for the attacker to reach the point without being captured by the defender. However, only the regions where exists  $j$  such that  $t_{Aj}(\mathbf{x}) < t_{D1}(\mathbf{x})$  or  $t_{D2}(\mathbf{x}) < t_{Aj}(\mathbf{x}) < t_{D3}(\mathbf{x})$  satisfy Definition 3 for ADR. Therefore, another type of the attacker's dominance region should exist inside  $\mathcal{M}_D$ . Before introducing this new type of the attacker's dominance region, we first investigate the properties of  $\mathcal{L}$ , the boundary formed by the intersections of isochrones.

In  $\mathcal{M}_D$ , let  $\mathcal{L}$  intersects with  $\partial\mathcal{M}_D$  at  $\mathbf{x}$ , and  $t$  is the time  $\mathcal{I}_A$  and  $\mathcal{I}_D$  intersect at  $\mathbf{x}$ . Boundary  $\mathcal{L}$  has the following properties:

- (1) If  $\mathbf{x} \in \mathcal{B}_I^D$  and  $t = t_{D3}(\mathbf{x})$  or  $\mathbf{x} \in \mathcal{B}_{II}^D$  and  $t = t_{D1}(\mathbf{x})$ ,  $\mathcal{L}$  can penetrate  $\partial\mathcal{M}_D$  because  $t_{D3}$  is continuous at any point on  $\mathcal{B}_I^D$  and  $t_{D1}$  is continuous at any point on  $\mathcal{B}_{II}^D$ .
- (2) If  $t = t_{D2}(\mathbf{x})$ ,  $\mathcal{L}$  is tangent to  $\partial\mathcal{M}_D$ ; otherwise, it is contradictory to the continuity of the reaching times.

The situation for  $\mathcal{L}$  intersecting with  $\partial\mathcal{M}_A$  is similar. Due to the continuity of  $t_{Aj}(\mathbf{x})$  and  $t_{Dk}(\mathbf{x})$ , the subscript  $j, k$  of  $t_{Aj}(\mathbf{x}) = t_{Dk}(\mathbf{x})$  will not change on  $\mathbf{x} \in \mathcal{L}$  unless  $\mathcal{L}$  intersects with  $\partial\mathcal{M}_A$  or  $\partial\mathcal{M}_D$ . In addition, the order of the attacker's and defender's reaching times also relates to  $\mathcal{L}$ , as stated below:

**Lemma 4.** Assume that  $t_{Aj} = t_{Dk}$  on part of  $\mathcal{L}$ , then the order of magnitude between  $t_{Aj}$  and  $t_{Dk}$  differs on two sides of  $\mathcal{L}$ .

*Proof.* Let the tangent vector of  $\mathcal{L}$  at  $\mathbf{x}$  be  $\mathbf{b}$ , while the normal vector  $\mathbf{n}$  is perpendicular to  $\mathbf{b}$ . The tangent vector exists when  $\mathcal{I}_A$  is not tangent to  $\mathcal{I}_D$ . Since the reach-

ing times of the attacker and defender equal along  $\mathcal{L}$ , the derivatives of the time with respect to the parameter  $t$  of  $\mathcal{L}$  are also equal:

$$\frac{dt_{Dk}(\mathbf{x}(t))}{dt} = \frac{dt_{Aj}(\mathbf{x}(t))}{dt}, \quad (35)$$

where  $\mathbf{x}(t) \in \mathcal{L}$ . The derivative can be expressed as

$$\frac{dt_{ij}(\mathbf{x}(t))}{dt} = \frac{d\mathbf{x}(t)}{dt} \frac{dt_{ij}(\mathbf{x}(t))}{d\mathbf{x}(t)} = \mathbf{b}^T \frac{dt_{ij}(\mathbf{x}(t))}{d\mathbf{x}(t)}. \quad (36)$$

Therefore, (35) can be rewritten as

$$\mathbf{b}^T \frac{dt_{Dk}(\mathbf{x}(t))}{d\mathbf{x}(t)} = \mathbf{b}^T \frac{dt_{Aj}(\mathbf{x}(t))}{d\mathbf{x}(t)}. \quad (37)$$

If the relative magnitude order between  $t_{Aj}$  and  $t_{Dk}$  remains unchanged, we may assume that  $t_{Aj}(\mathbf{x}(t)) = t_{Dk}(\mathbf{x}(t))$  and  $t_{Aj}(\mathbf{x}(t) + \beta\mathbf{n}) > t_{Dk}(\mathbf{x}(t) + \beta\mathbf{n})$  on both sides of  $\mathcal{L}$ , for  $|\beta|$  smaller than a given constant. Then we can similarly derive that

$$\mathbf{n}^T \frac{dt_{Dk}(\mathbf{x}(t))}{d\mathbf{x}(t)} = \mathbf{n}^T \frac{dt_{Aj}(\mathbf{x}(t))}{d\mathbf{x}(t)}. \quad (38)$$

Therefore,  $\frac{dt_{Dk}(\mathbf{x}(t))}{d\mathbf{x}(t)} = \frac{dt_{Aj}(\mathbf{x}(t))}{d\mathbf{x}(t)}$  at any points on  $\mathcal{L}$ .

However, it can be verified from (17) that  $\frac{dt_{Aj}(\mathbf{x}_A)}{d\mathbf{x}_A}$  and  $\frac{dt_{Dk}(\mathbf{x}_D)}{d\mathbf{x}_D}$  are parallel if and only if  $\mathcal{I}_A$  and  $\mathcal{I}_D$  circumscribe or inscribe, which is satisfied for finite times, meaning that  $\frac{dt_{Dk}(\mathbf{x}(t))}{d\mathbf{x}(t)} = \frac{dt_{Aj}(\mathbf{x}(t))}{d\mathbf{x}(t)}$  for finite times. Hence, on two sides separated by  $\mathcal{L}$ , the order of the attacker's and defender's reaching times differs.  $\square$

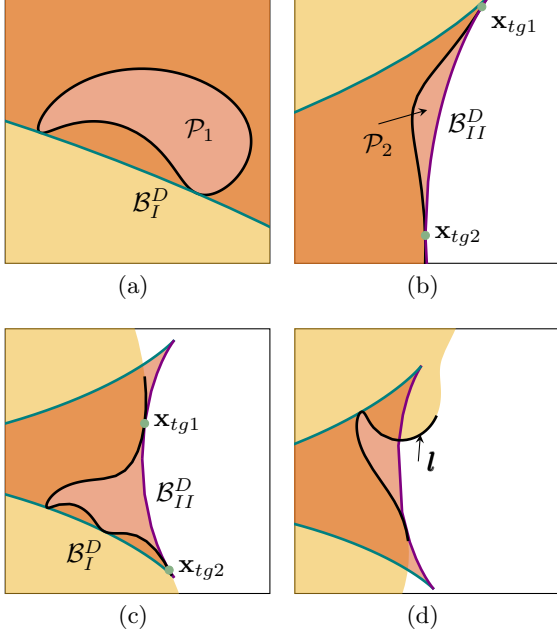


Fig. 5. Illustrations for the third type of the attacker's dominance region

Next, we introduce the definition of the third type of the attacker's dominance region.

**Definition 4.** The third type of the attacker's dominance region  $\mathcal{R}_{III}$  are regions in  $\mathcal{M}_D$  that  $t_{D1}(\mathbf{x}) < t_A(\mathbf{x}) < t_{D2}(\mathbf{x})$  or  $t_{D1}(\mathbf{x}) < t_{A1}(\mathbf{x}) < t_{D2}(\mathbf{x})$ , and will continuously contract to a point as  $u_A$  decreases.

As  $\mathcal{R}_{III}$  continuously contract to a point, all the points in  $\mathcal{R}_{III}$  will be in  $\mathcal{R}_I(u_A^*) \cup \mathcal{R}_{II}(u_A^*)$  for a certain  $u_A^* < u_{Am}$ , which means the attacker can reach a point in  $\mathcal{R}_{III}$  when it is not in  $\mathcal{I}_D$ . There are regions in  $\mathcal{M}_D$  with different combinations of the relationships between  $t_{Aj}(\mathbf{x})$  and  $t_{Dk}(\mathbf{x})$  satisfying  $t_{D1}(\mathbf{x}) < t_{Aj}(\mathbf{x}) < t_{D2}(\mathbf{x})$ ,  $j \in \{0, 1\}$ . However, there may not exist a strategy for the attacker to reach some of these regions when they are outside  $\mathcal{I}_D$ . Next, two special types of region that belong to  $\mathcal{R}_{III}$  are given.

**Theorem 2.** The region that satisfies either of the following two conditions is the third type of attacker's dominance region.

- (1) the boundary of the region consists solely of intersections of isochrones between the first and second circumscribing times  $t_{o1}$  and  $t_{o2}$ , and  $\|\mathbf{x}_{Ac}(t) - \mathbf{x}_{Dc}(t)\|_2 > r_{Dc}(t)$  during  $[t_{o1}, t_{o2}]$ .
- (2) the boundary of the region consists solely of  $\mathcal{B}_{II}^D$  and part of  $\mathcal{L}$  where  $t_{A1}(\mathbf{x}) = t_{D2}(\mathbf{x})$  for  $\mathbf{x} \in \mathcal{M}_A$  and  $t_A(\mathbf{x}) = t_{D2}(\mathbf{x})$  for  $\mathbf{x} \in \mathbb{R}^2 \setminus \mathcal{M}_A$ .

*Proof.* For simplicity, we use  $t_A(\mathbf{x})$  to refer to both  $t_A(\mathbf{x})$  for  $\mathbf{x} \in \mathbb{R}^2 \setminus \mathcal{M}_A$  and  $t_{A1}(\mathbf{x})$  for  $\mathbf{x} \in \mathcal{M}_A$  as there is no

need to distinguish them in the proof.

We first discuss the region that satisfies condition 1), and denote it as  $\mathcal{P}_1$ , as shown in Fig. 5(a).

The circumscribing times  $t_{o1}$  and  $t_{o2}$  are determined by the functions  $o(t)$  and  $p_{out}(t)$  given in (16), which are continuous with respect to  $u_A$  and  $t$ . Therefore, as  $u_A$  decreases,  $t_{o1}(u_A)$  and  $t_{o2}(u_A)$  are continuous before  $t_{o1}(u_A) = t_{o2}(u_A)$ .

As  $u_A$  decreases, the center of  $\mathcal{I}_A(t)$  remains unchanged, while the radius decreases. So  $t_{o1}(u_A) \geq t_{o1}(u_{Am})$ ,  $t_{o2}(u_A) \leq t_{o2}(u_{Am})$ . Moreover, since  $\|\mathbf{x}_{Ac}(t) - \mathbf{x}_{Dc}(t)\|_2 > r_{Dc}(t)$  during  $[t_{o1}(u_{Am}), t_{o2}(u_{Am})]$ ,  $\mathcal{I}_A$  do not intersect with  $\mathcal{I}_D$  if  $u_A = 0$ , indicating that there exists a value  $u_A^*$  such that  $\mathcal{I}_A$  is tangent to  $\mathcal{I}_D$  from outside only once during  $[t_{o1}(u_{Am}), t_{o2}(u_{Am})]$  at the time  $t_{o1}(u_A^*) = t_{o2}(u_A^*)$ .  $\mathcal{P}_1$  contracts to the tangent point and then vanishes as  $u_A$  decreases. Therefore,  $\forall \mathbf{x} \in \mathcal{P}_1, \exists u_A \in [u_A^*, u_{Am}]$  s.t.  $\mathbf{x} \in \mathcal{R}_{II}(u_A) \cup \mathcal{R}_I(u_A)$ .

$\mathcal{P}_1$  contains points that belong to a subset of  $\mathcal{I}_A(t)$  that are inside  $\mathcal{I}_D(t)$ , which means  $t_{D1} < t_A < t_{D2}$  or  $t_{D3} < t_A$  at these points. If  $t_A(\mathbf{x}) > t_{D3}(\mathbf{x})$ , then  $\mathbf{x}$  is contained in  $\mathcal{I}_D(t)$  for  $t > t_A(\mathbf{x})$ , which is contradictory to the existence of  $u_A^*$  given in the last paragraph. Therefore,  $t_{D1} < t_A < t_{D2}$  inside  $\mathcal{P}_1$ .  $\mathcal{P}_1$  is the third type of the attacker's dominance region.

Next, we analyse the region satisfying the second condition, as shown in Fig. 5(b), denoted as  $\mathcal{P}_2$ . The intersections of  $\mathcal{B}_{II}^D$  and  $\mathcal{L}$  are tangent points  $\mathbf{x}_{tg1}$  and  $\mathbf{x}_{tg2}$ , where  $t_A(\mathbf{x}_{tgi}) = t_{D2}(\mathbf{x}_{tgi}) = t_{D3}(\mathbf{x}_{tgi})$ . Since the boundary of the region on other side of  $\mathcal{L}$  contains curve where  $t_A(\mathbf{x}) = t_{D3}(\mathbf{x})$ , the region satisfies  $t_{D2}(\mathbf{x}) < t_A(\mathbf{x}) < t_{D3}(\mathbf{x})$ . From Lemma 4, we can conclude that  $t_{D1}(\mathbf{x}) < t_A(\mathbf{x}) < t_{D2}(\mathbf{x})$  in  $\mathcal{P}_2$ .

$\mathbf{x}_{tg1}$  and  $\mathbf{x}_{tg2}$  change continuously as  $u_A$  decreases from  $u_{Am}$ . Otherwise,  $\mathbf{x}_{tg1}$  vanishes or jumps before  $\mathbf{x}_{tg1}(u_A) = \mathbf{x}_{tg2}(u_A)$ , and all points in  $\mathcal{P}_2$  abruptly change from  $t_A(\mathbf{x}) < t_{D2}(\mathbf{x})$  to  $t_A(\mathbf{x}) > t_{D2}(\mathbf{x})$ , indicating that  $t_A(\mathbf{x})$  in  $\mathcal{P}_2$  does not change continuously with respect to  $u_A$ . However,  $\mathcal{P}_2$  is not a null set if  $\mathbf{x}_{tg1} \neq \mathbf{x}_{tg2}$ . That is contradictory to the continuity of  $t_A(\mathbf{x})$ .

As  $u_A$  decreases, the radii of the attacker's isochrones decrease, so  $t_{A1}(\mathbf{x})$  and  $t_A(\mathbf{x})$  increase. So,  $\mathbf{x}_{tgi}$  moves on  $\mathcal{B}_{II}^D$  into parts that  $t_A < t_{D2}$ , which is between  $\mathbf{x}_{tg1}$  and  $\mathbf{x}_{tg2}$ . Similarly, the part of  $\mathcal{L}$  where  $t_A = t_{D2}$  contracts into  $\mathcal{P}_2$  as  $u_A$  decreases. Consequently, the area of  $\mathcal{P}_2$  continuously decreases to zero as  $u_A$  decreases.  $\forall \mathbf{x} \in \mathcal{P}_2, \exists u_A < u_{Am}$  s.t.  $\mathbf{x} \in \partial \mathcal{R}_{III}(u_A)$ , that is  $\mathbf{x} \in \mathcal{R}_{II}(u_A) \cup \mathcal{R}_I(u_A)$ .

□

Regions where the conditions in Theorem 2 are satisfied are guaranteed to contract to a point. However, regions that do not meet the conditions are also probably reachable for the attacker. For instance, as illustrated in Fig. 5(c), there exists a region with its boundary consisting of  $\mathcal{B}_{II}^D$ , part of  $\mathcal{L}$  where  $t_A(\mathbf{x}) = t_{D1}(\mathbf{x})$  or  $t_A(\mathbf{x}) = t_{D2}(\mathbf{x})$ , and the intersections of  $\mathcal{L}$  and  $\partial\mathcal{M}_D$  are tangent points. As  $u_A$  decreases, the number of circumscribing times increase from one to three. The region will transform into two  $\mathcal{R}_{III}$ , satisfying two conditions in Theorem 2 respectively. In fact, all points in this region is reachable for the attacker. However, there is still no criterion to guarantee that this region are reachable. For example, there may exist  $t$  such that  $\|\mathbf{x}_{Ac}(t) - \mathbf{x}_{Dc}(t)\|_2 < r_{Dc}(t)$ , which means the attacker's isochrones will eventually be contained in the defender's isochrones as  $u_A$  decreases. Then,  $\mathbf{x}_{Ac}(t)$  is unreachable for the attacker.

What's more, there are regions where  $t_{D1} < t_A < t_{D2}$  is satisfied but the attacker cannot reach at. For instance, when the attacker is at rest at start, and the part of  $\mathcal{L}$  that  $t_{A1}(\mathbf{x}) = t_{D1}(\mathbf{x})$  (denoted as  $\mathcal{I}$ ) intersect with  $\mathcal{B}_{II}^D$ , as shown in Fig. 5(d),  $\mathcal{I}$  will move into  $\mathcal{R}_I \cup \mathcal{R}_{II}$  as  $u_A$  decreases. Unlike the boundary formed between two circumscribing times, this part of boundary will not vanish. Instead, it will only gradually approach  $\mathbf{x}_{A0}$ .

It can be inferred from the Definition 3 that  $\mathcal{R}_{III}$  is not contained in  $\mathcal{R}_I \cup \mathcal{R}_{II}$ . Therefore, we extend the typical attacker's dominance region into a larger area, meaning that the attacker can reach the outside of  $\mathcal{R}_I \cup \mathcal{R}_{II}$  with a smaller  $u_A$ .

Now, we propose the **multiple reachable region (MRR) strategy** for the attacker to reach  $\mathcal{R}_{III}$ . In order for the attacker to reach  $\mathbf{x} \in \mathcal{R}_{III}$  when the defender can not reach the point, the attacker needs to adopt the acceleration magnitude  $\hat{u}_A$  which enables  $t_A(\mathbf{x}, \hat{u}_A) = t_{D2}(\mathbf{x})$ . To this end, we first calculate  $t_{D2}(\mathbf{x})$  using Algorithm 1. Then, the acceleration  $\hat{u}_A$  is determined by solving:

$$\frac{\hat{u}_A}{\mu} \left( t_{D2}(\mathbf{x}) - \frac{1 - e^{-\mu t_{D2}(\mathbf{x})}}{\mu} \right) = \|\mathbf{x} - \mathbf{x}_{Ac}(t_{D2}(\mathbf{x}))\|_2.$$

We provide illustrations of the complete attacker's dominance region in Fig. 6. If the attacker is static at start,  $\mathcal{R}_{II}$  is region that it can not reach in a straight line in ADR. In Fig. 6(a), isochrones circumscribe and inscribe for one time, and  $\mathcal{R}_{III}$  is a connected region. In Fig. 6(c), isochrones circumscribe for three times before inscribe. The area isolated in  $\mathcal{R}_I \cup \mathcal{R}_{II}$  corresponds to a part of  $\mathcal{R}_{III}$ , satisfying the first condition given in Theorem 2, while the other  $\mathcal{R}_{III}$  region satisfies the second condition.

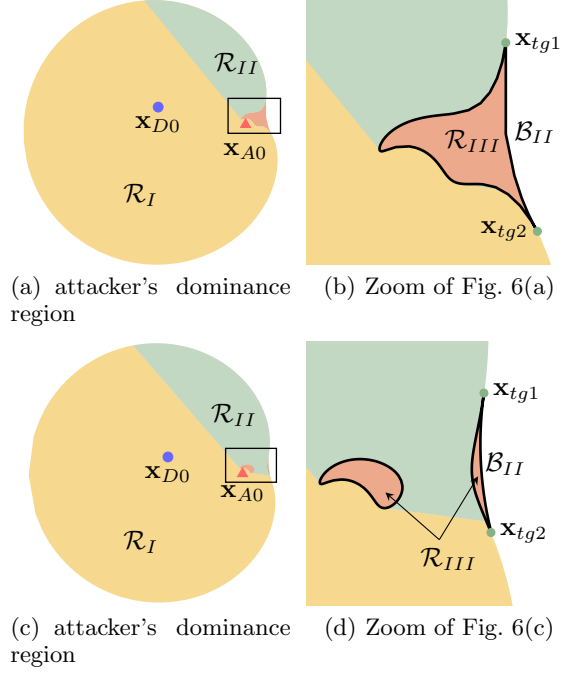


Fig. 6. Illustrations about attacker's dominance region. The attacker can reach  $\mathcal{R}_I$  without being caught by the defender, while it might be caught before reaching  $\mathcal{R}_{II}$ . To reach  $\mathcal{R}_{III}$ , the attacker has to change strategy, such as adopting a smaller acceleration.

$\mathcal{R}_{III}$  can only be reached by the attacker with strategy different from the optimal strategy in (12). This indicates that (12) derived from Maximum Principle does not hold when the attacker tries to enter or pass  $\mathcal{R}_{III}$ . In the following part, we will discuss about the condition for a strategy to be optimal and the influence brought by the existence of  $\mathcal{R}_{III}$ .

### 3.4 Necessary Condition for the Optimal Strategy

Denote the strategy of reaching the point closest to the target on  $\mathcal{L}$  with  $u_i = u_{im}$  and constant  $\theta_i$  as **strategy I**. According to the Maximum Principle,  $\max_{u_D, \theta_D} \min_{u_A, \theta_A} H = H(\mathbf{x}_i, \theta_i^*, u_i^*, \lambda, \gamma, t) = 0$  is a necessary condition for strategy I to be optimal.

Next, we derive a sufficient condition related to players' reaching times for  $H = 0$  to be satisfied at the local minimal points on  $\mathcal{L}$ .

**Theorem 3.**  $H(\mathbf{x}_i, \theta_i^*, u_i^*, \lambda, \gamma, t) = 0$  holds at local minimal point  $\mathbf{x} \in \mathcal{L}$  if  $t_{Dk}(\mathbf{x}) = t_{Aj}(\mathbf{x})$ ,  $k \in \{0, 1, 3\}$ ,  $j \in \{0, 1, 3\}$  or  $t_{D2}(\mathbf{x}) = t_{A2}(\mathbf{x})$ , and the gradients of  $t_{Dk}(\mathbf{x})$  and  $t_{Aj}(\mathbf{x})$  given in (17) exist at  $\mathbf{x}$ .

*Proof.* We first define an auxiliary problem for the proof.

Local Minimal (Maximal) Time Problem: Consider a damped double integrator player  $i$ . Given the initial state

$\mathbf{x}_{i0}$ ,  $\mathbf{v}_{i0}$  and target position  $\mathbf{x}$ , find the local minimal (maximal) time for player  $i$  to reach  $\mathbf{x}$ .

To solve the auxiliary problem by optimal control theory, the payoff function is defined as  $J = t_f$  for reaching a point in the local minimal time and  $J = -t_f$  for local maximal time. For player  $i$ , the Hamiltonian is:

$$H = \kappa_{i1}v_{ix} + \kappa_{i2}v_{iy} + \kappa_{i3}(-\mu v_{ix} + u_i \cos \theta_i) + \kappa_{i4}(-\mu v_{iy} + u_i \sin \theta_i), \quad (39)$$

where  $\kappa_{im}, m \in \{1, 2, 3, 4\}$  is the co-state. At  $t = t_f$ ,  $\kappa_{i3} = \kappa_{i4} = 0$ . Denote  $[\kappa_{i1}, \kappa_{i2}]^T = \kappa_i$ , according to [4],

$$\kappa_i(t) = \pm \frac{\partial t_i(\mathbf{x}, \mathbf{x}_i(t), \mathbf{v}_i(t))}{\partial \mathbf{x}_i(t)}, \quad \dot{\kappa}_i(t) = 0,$$

where  $t_i(\mathbf{x}, \mathbf{x}_i(t), \mathbf{v}_i(t))$  is the time to reach  $\mathbf{x}$  for player  $i$  at  $\mathbf{x}_i(t)$  with velocity  $\mathbf{v}_i(t)$ , the positive sign of  $\kappa_i$  corresponds to the local minimal time and the minus sign corresponds to the local maximal time. As the co-state  $\kappa_i$  is constant, we can get

$$\kappa_i(t) = \pm \frac{\partial t_i(\mathbf{x}, \mathbf{x}_{i0}, \mathbf{v}_{i0})}{\partial \mathbf{x}_{i0}}, \quad \forall t \in [0, t_f]. \quad (40)$$

Next, we verify that  $t_{Dk}(\mathbf{x})$  and  $t_{Aj}(\mathbf{x})$ ,  $i, j \in \{0, 1, 2, 3\}$  are solutions to this problem. By taking the derivative of (13) with respect to  $\mathbf{x}$  and  $\mathbf{x}_{i0}$ ,

$$\frac{\partial t_i(\mathbf{x}, \mathbf{x}_{i0}, \mathbf{v}_{i0})}{\partial \mathbf{x}} + \frac{\partial t_i(\mathbf{x}, \mathbf{x}_{i0}, \mathbf{v}_{i0})}{\partial \mathbf{x}_{i0}} = 0.$$

With the gradient for the reaching time given in (17), the Hamiltonian defined in (39) can be formulated as

$$\begin{aligned} H &= \pm \mathbf{v}_{if}^T \frac{\partial t_i(\mathbf{x}, \mathbf{x}_{i0}, \mathbf{v}_{i0})}{\partial \mathbf{x}_{i0}} \\ &= \mp \mathbf{v}_{if}^T \frac{1}{v_{ix} \cos \theta_i + v_{iy} \sin \theta_i} [\cos \theta_i, \sin \theta_i]^T \\ &= \mp 1. \end{aligned} \quad (41)$$

The gradient of  $t_i(\mathbf{x})$  given in (17) exists if  $\mathbf{x}$  is not the tangent point of  $\mathcal{L}$  and  $\partial \mathcal{M}_A$  or  $\partial \mathcal{M}_D$ . For solutions  $t_{i2}(\mathbf{x})$ ,  $H = 1$ . For other reaching times,  $H = -1$ . This can be understood by regarding  $t_{i2}(\mathbf{x})$  as a local maximal time to reach  $\mathbf{x}$  because for  $t \in [t_{i1}(\mathbf{x}), t_{i2}(\mathbf{x})]$ ,  $\mathbf{x}$  is in the isochrones, but for  $t \in [t_{i2}(\mathbf{x}), t_{i3}(\mathbf{x})]$ , it is outside the isochrones. Based on the sign of the Hamiltonian, the reaching times can be divided into two categories, each combination of the attacker and defender's reaching times from the same category satisfies

$$\mathbf{v}_{Af}^T \frac{\partial t_A(\mathbf{x}, \mathbf{x}_{A0}, \mathbf{v}_{A0})}{\partial \mathbf{x}_{A0}} - \mathbf{v}_{Df}^T \frac{\partial t_D(\mathbf{x}, \mathbf{x}_{D0}, \mathbf{v}_{D0})}{\partial \mathbf{x}_{D0}} = 0. \quad (42)$$

Now consider the reach-avoid game in this paper, the local minimal point  $\mathbf{x}_f$  on the boundary of  $\mathcal{R}_I$  and  $\mathcal{R}_{II}$  satisfies:

$$\begin{aligned} &\frac{d}{d\mathbf{x}_f} \sqrt{x_f^2 + y_f^2} \\ &+ \sigma \left( \frac{\partial t_A(\mathbf{x}_f, \mathbf{x}_{A0}, \mathbf{v}_{A0})}{\partial \mathbf{x}_f} - \frac{\partial t_D(\mathbf{x}_f, \mathbf{x}_{D0}, \mathbf{v}_{D0})}{\partial \mathbf{x}_f} \right) = 0, \end{aligned} \quad (43)$$

where  $\sigma$  is the Lagrange multiplier. Equation (43) can be rewritten as

$$\begin{aligned} &\frac{d}{d\mathbf{x}_f} \sqrt{x_f^2 + y_f^2} \\ &- \sigma \left( \frac{\partial t_A(\mathbf{x}_f, \mathbf{x}_{A0}, \mathbf{v}_{A0})}{\partial \mathbf{x}_{A0}} - \frac{\partial t_D(\mathbf{x}_f, \mathbf{x}_{D0}, \mathbf{v}_{D0})}{\partial \mathbf{x}_{D0}} \right) = 0. \end{aligned} \quad (44)$$

Define  $\hat{\lambda}$  and  $\hat{\gamma}$  as

$$\begin{aligned} \hat{\lambda} &= [\hat{\lambda}_1, \hat{\lambda}_2]^T = -\sigma \frac{\partial t_D(\mathbf{x}_f, \mathbf{x}_{D0}, \mathbf{v}_{D0})}{\partial \mathbf{x}_{D0}}, \\ \hat{\gamma} &= [\hat{\gamma}_1, \hat{\gamma}_2]^T = \sigma \frac{\partial t_A(\mathbf{x}_f, \mathbf{x}_{A0}, \mathbf{v}_{A0})}{\partial \mathbf{x}_{A0}}. \end{aligned} \quad (45)$$

We now verify that  $\hat{\lambda}$  and  $\hat{\gamma}$  are the co-states of the position for this reach-avoid game. To this end, we demonstrate that  $\hat{\lambda}$  and  $\hat{\gamma}$  satisfy  $H = 0$ , with  $H$  given in (7), and  $\hat{\lambda} = \frac{\partial \Phi}{\partial \mathbf{x}_D^T} + \nu \frac{\partial g}{\partial \mathbf{x}_D^T}$ ,  $\hat{\gamma} = \frac{\partial \Phi}{\partial \mathbf{x}_A^T} + \nu \frac{\partial g}{\partial \mathbf{x}_A^T}$  (corresponding to (10) and (11)), which can be used to determine  $\lambda_1, \lambda_2, \gamma_1, \gamma_2$ .

At  $t = t_f$ ,  $\lambda_3 = \lambda_4 = 0$  and  $\gamma_3 = \gamma_4 = 0$ , so  $H = \lambda_1 v_{Dxf} + \lambda_2 v_{Dyf} + \gamma_1 v_{Axf} + \gamma_2 v_{Ayf}$ . If  $t_A(\mathbf{x}_f, \mathbf{x}_{A0}, \mathbf{v}_{A0})$  and  $t_D(\mathbf{x}_f, \mathbf{x}_{D0}, \mathbf{v}_{D0})$  are the solutions of auxiliary problem, by substituting (45) into (42) we can obtain that

$$\hat{\gamma}^T \mathbf{v}_{Af} + \hat{\lambda}^T \mathbf{v}_{Df} = 0, \quad (46)$$

which is equivalent to  $H = 0$ .

According to (10), (11) and (17), let  $\sigma = |\nu|(v_{Dxf} \cos \theta_D + v_{Dyf} \sin \theta_D)$ , we have  $\hat{\lambda} = \frac{\partial \Phi}{\partial \mathbf{x}_D^T} + \nu \frac{\partial g}{\partial \mathbf{x}_D^T}$ .

Then, from (10) and (11),  $\gamma_1$  and  $\gamma_2$  can be determined by  $\lambda_1 + \gamma_1 = \frac{x_f}{\sqrt{x_f^2 + y_f^2}}$  and  $\lambda_2 + \gamma_2 = \frac{y_f}{\sqrt{x_f^2 + y_f^2}}$ . It can be inferred from (44) that  $\hat{\lambda}$  and  $\hat{\gamma}$  also satisfy this relationship.

According to (7), (10), and (11), the players' strategies

of the reach-avoid game are given by

$$\begin{aligned}
\theta_A^* &= \arg \min_{\theta_A} H \\
&= \arg \min_{\theta_A} \sigma \frac{\partial t_A(\mathbf{x}_f, \mathbf{x}_{A0}, \mathbf{v}_{A0})}{\partial \mathbf{x}_{A0}^T} [\cos \theta_A, \sin \theta_A]^T, \\
\theta_D^* &= \arg \max_{\theta_D} H \\
&= \arg \min_{\theta_D} \sigma \frac{\partial t_D(\mathbf{x}_f, \mathbf{x}_{D0}, \mathbf{v}_{D0})}{\partial \mathbf{x}_{D0}^T} [\cos \theta_D, \sin \theta_D]^T.
\end{aligned} \tag{47}$$

For minimal reaching time, where  $\frac{d}{dt}(\|\mathbf{x}_f - \mathbf{x}_{Dc}(t_f)\|_2 - r_{Dc}(t_f)) < 0$ , we derive

$$v_{Dxf} \cos \theta_D + v_{Dyf} \sin \theta_D > 0,$$

which means  $\sigma > 0$ , the strategies are the optimal strategy for local minimal time problem. Similarly, if both player's reaches the terminal position at locally maximal time, the strategies are the optimal strategy for local maximal time problem.

Therefore,  $\hat{\lambda}$  and  $\hat{\gamma}$  are solutions of the position co-states. For local minimal point  $\mathbf{x} \in \mathcal{L}$  that  $t_{Dk}(\mathbf{x}) = t_{Aj}(\mathbf{x})$ ,  $k \in \{0, 1, 3\}$ ,  $j \in \{0, 1, 3\}$  or  $t_{D2}(\mathbf{x}) = t_{A2}(\mathbf{x})$ ,  $H = 0$  is satisfied along the trajectory.  $\square$

When  $H = 0$  is not satisfied at the local minimal point on  $\mathcal{L}$ , there exists a strategy for the attacker to achieve better performance, i.e. being captured closer to the target or reach the target. Let's first consider the part of  $\mathcal{L}$  where  $t_{D2} = t_{A1}$ . On one side of  $\mathcal{L}$ ,  $t_{D2} < t_{A1} < t_{D3}$ , which is in  $\mathcal{R}_I \cup \mathcal{R}_{II}$  by definition. On the other side,  $t_{D1} < t_{A1} < t_{D2}$ . If the local minimal point  $\mathbf{x}$  is on this part of  $\mathcal{L}$ , the attacker can adopt a smaller  $u_A$  to make  $t_{D2}(\mathbf{x}) < t_{A1}(\mathbf{x})$  and therefore let the point belong to  $\mathcal{R}_I \cup \mathcal{R}_{II}$ , which means the attacker may have strategy to get closer to the target. The part of  $\mathcal{L}$  where  $t_{D2} = t_{A1}$  is similar.

As for the part of  $\mathcal{L}$  where  $t_{D2} = t_{A3}$ , if  $t_{A1} < t_{D1}$ , it is in  $\mathcal{R}_I \cup \mathcal{R}_{II}$  regardless of the relation between  $t_{D2}$  and  $t_{A3}$ . Therefore, a better target point must exist on  $\mathcal{L}$ . If  $t_{A1} > t_{D1}$ , then  $t_{D2} < t_{A3} < t_{D3}$  on the one side, which belongs to  $\mathcal{R}_I \cup \mathcal{R}_{II}$ , while  $t_{D1} < t_{A1} < t_{A2} < t_{A3} < t_{D2}$  on the other side, where the attacker can increase  $t_{A3}$  by adopting smaller  $u_A$  and possibly make part of this region belong to  $\mathcal{R}_I \cup \mathcal{R}_{II}$ . So, the attacker may have strategy to have better performance.

For the part of  $\mathcal{L}$  where  $t_{D1} = t_{A2}$  or  $t_D = t_{A2}$ , on both sides of  $\mathcal{L}$ ,  $t_{A1} < \min t_D$ , so both sides are in  $\mathcal{R}_I \cup \mathcal{R}_{II}$ .

For the part of  $\mathcal{L}$  where  $t_{D3} = t_{A2}$ , the side where  $t_{D2} < t_{A2} < t_{D3}$  is in  $\mathcal{R}_I \cup \mathcal{R}_{II}$  by definition, while the other side where  $t_{D3} < t_{A2}$  may be outside the ADR. However,  $t_{A2}$  decreases as the attacker adopts a smaller

$u_A$ , which means  $\mathcal{L}$  moves into region that  $t_{D3} < t_{A2}$ , so the attacker has a better target point by adopting smaller  $u_A$ .

All the equations in the proof of Theorem 3 are derived under the assumption that the optimal strategy employs  $u_{im}$ . So, if the attacker adopts different strategy to reach the optimal point, such as MRR strategy,  $H = 0$  does not hold.

In summary,  $H = 0$  does not hold at local minimal points where  $t_{D2} = t_{Aj}$ ,  $j \in \{0, 1, 3\}$ , or  $t_{Dk} = t_{A2}$ ,  $k \in \{0, 1, 3\}$ . They are either in  $\mathcal{R}_I \cup \mathcal{R}_{II}$  or regions that can be changed into ADR with smaller  $u_A$ , thus a better strategy may exist for the attacker. The boundary of  $\mathcal{R}_{III}$  contains some of these points and extend the attacker's dominance region.

### 3.5 A Special Case: Players Initially at Rest

In this section, we discuss about the case when both the attacker and defender are at rest at  $t = 0$ . Then, each player's isochrones will not overlap, i.e.  $t_{is} = 0$ . Denote the ratio of the maximum acceleration as  $\alpha = \frac{u_{Am}}{u_{Dm}}$ . We investigate the properties of the attacker's dominance region and the local minimal point under this condition.

**Lemma 5.** If players are initially at rest, the boundary of the attacker's dominance region is an Apollonius circle, with center at  $\mathbf{x}_b = \frac{1}{1-\alpha^2}(\mathbf{x}_{A0} - \alpha^2 \mathbf{x}_{D0})$ , and radius  $r_b = \frac{\alpha}{1-\alpha^2} \|\mathbf{x}_{A0} - \mathbf{x}_{D0}\|_2$ .

*Proof.* The isochrones in this situation can be simplified to

$$\begin{aligned}
r_{ic} &= \frac{u_{im}}{\mu} \left( t - \frac{1 - e^{-\mu t}}{\mu} \right), \\
x_{ic} &= x_{i0}, \quad y_{ic} = y_{i0}.
\end{aligned} \tag{48}$$

Therefore, the isochrones of the attacker or defender are concentric circles, with the ratio of the radii is  $\frac{r_{Ac}}{r_{Dc}} = \frac{u_{Am}}{u_{Dm}} = \alpha$ .

The dominance boundary is formed by the set of intersections of isochrones, i.e.  $\{\mathbf{x} \in \mathbb{R}^2 \mid \frac{\|\mathbf{x} - \mathbf{x}_{A0}\|}{\|\mathbf{x} - \mathbf{x}_{D0}\|} = \alpha\}$ , which is equivalent to the definition of Apollonius circle.  $\square$

**Theorem 4.** In defender-winning scenarios, if the attacker and defender are at rest at  $t = 0$ , the minimal point is unique and satisfies  $H = 0$ .

*Proof.* The target is outside the ADR in defender-winning scenarios. The uniqueness of the minimal point is ensured by the convexity of the Apollonius circle.

Because  $\mathcal{I}_i$  do not overlap, the minimal time to reach any point  $\mathbf{x} \in \mathbb{R}^2$  is continuous and uniquely determined.

According to Theorem 3, the minimal point satisfies  $H = 0$ .

□

Therefore, if the players are initially at rest, the optimal strategy is to reach the minimal point on the Apollonius circle, which is the intersection of the circle and line connecting the target and the circle's center.

## 4 Simulations

This section conducts simulations to demonstrate the effectiveness of our strategy, followed by special cases that the optimal point exists in  $\mathcal{R}_{III}$  or the attacker needs to cross  $\mathcal{R}_{III}$  to show the necessity to introduce the third type of the attacker's dominance region. The parameters are set as follow:  $u_A = 1, u_D = 2, \mu = 1$ , the target is at  $[0, 0]^T$ . All our simulations are produced by Matlab2023a.

First, we conducted three experiments to illustrate the effectiveness of strategy I. In each game, the minimal point on ADR's boundary satisfies  $H = 0$ . The attacker and defender adopt strategy I, denoted as  $\theta_i^*$ , or pure-pursuit strategy, i.e.  $\theta_A(t) = \arctan \frac{y_{At}}{x_{At}} + m\pi$  and  $\theta_D(t) = \arctan \frac{y_{Dt} - y_{At}}{x_{Dt} - x_{At}} + n\pi$ . The acceleration  $u_i$  of each player equals to the maximum acceleration  $u_{im}$ . The attacker will also check whether it can reach the target without being captured. Once the attacker can, it will adopt the corresponding strategy to reach the target.

The first case's initial states are set as follow:  $x_{A0} = -2, y_{A0} = 3, x_{D0} = -3, y_{D0} = -2, v_{Ax0} = -1, v_{Ay0} = 0, v_{Dx0} = 0, v_{Dy0} = 2$ . The results are shown in Fig. 7. Red and blue lines are the trajectories of the attacker and the defender adopting open loop control with  $(\theta_A^*, \theta_D^*)$  obtained using strategy I under the initial states. The exact attacker and defender's trajectories of different strategies are pink and green dashed lines. The attacker's initial positions are marked with red triangles, while the defender's initial positions are blue dots. The target is marked with green dot. The terminal positions of the attacker and the defender are marked with red and blue stars. Fig. 7(d) shows the distance between the attacker and the defender. Fig. 7(e) shows the distance between the attacker and the target.

If both the attacker and the defender apply strategy I, the optimal terminal point  $\mathbf{x}_f^*$  does not change according to time, as shown in Fig. 7(a). In Fig. 7(b), the attacker applies pure pursuit strategy, while the defender applies strategy I, the game terminates at the point that is further from the target than  $\mathbf{x}_f^*$ , which means attacker's different strategy leads to a worse result for the attacker. If the defender applies pure pursuit strategy, while the attacker applies strategy I, the attacker

successfully reaches the target before being captured, as shown in Fig. 7(c). This demonstrates that if the defender changes its strategy unilaterally, the terminal distance to the target will decrease.

The second case's initial states are set as:  $x_{A0} = 1, y_{A0} = -0.1, x_{D0} = 1.2, y_{D0} = 0.1, v_{Ax0} = 0, v_{Ay0} = 0, v_{Dx0} = -0.5, v_{Dy0} = -1$ . The results are shown in Fig. 8. By comparing the distance to target when captured, as shown in Fig. 8(e), we concluded that either side change its strategy from strategy I, the result becomes worse for that player.

We carry out the third case under the initial states that players are at rest, i.e.  $v_{ix0} = 0, v_{iy0} = 0$ . Their initial positions are as follow:  $x_{A0} = -0.6, y_{A0} = 0.1, x_{D0} = -0.8, y_{D0} = -0.2$ . The results are shown in Fig. 9. The attacker dominance region is an Apollonius circle with the minimal point satisfying  $H = 0$ . The optimal point doesn't change with time if the attacker and the defender adopt strategy I. If the defender changes to pure-pursuit strategy, the payoff becomes worse for the defender, and vice versa.

Then we carry out two simulations of special cases that the minimal point in  $\mathcal{R}_{III}$  or the attacker has to cross  $\mathcal{R}_{III}$  to reach the optimal point. In these cases, strategy I is not the optimal strategy. the attacker can achieve better performance by adopting MRR strategy or the defender can capture the attacker before they reach the local minimal point if the attacker adopts strategy I.

In the first case, the real minimal point is in  $\mathcal{R}_{III}$ . We first simulate the situation that both the attacker and the defender ignore  $\mathcal{R}_{III}$ . That is, both the attacker and the defender adopt strategy I to reach the minimal point in  $\mathcal{R}_I \cup \mathcal{R}_{II}$ . The initial states are set as follow:  $x_{A0} = -0.3457, y_{A0} = 0.0517, x_{D0} = -0.6728, y_{D0} = -0.0455, v_{Ax0} = 0.0862, v_{Ay0} = 0.0338, v_{Dx0} = 1.6534, v_{Dy0} = 0.0907$ . In this case, the optimal point changes with time, which is illustrated in Fig. 10. In Fig. 10(c) and 10(d), at  $t=0.045s$  and  $t=0.1075s$ , the minimal point changes from its previous position which is marked with gray star, to a new position which is marked with green star. The boundaries of ADR at different times are drawn as gray curves. If the attacker and the defender apply strategy I, at the minimal point, the distance to target will not change with time. However, another local minimal point will become closer to the target and replace the current minimal point after two distances become the same.

We then simulate the situation that the attacker adopts MRR strategy to reach the optimal point in  $\mathcal{R}_{III}$ , while the defender reaches the same point in maximum acceleration. The results are shown in Fig. 11. If both the attacker and defender adopt strategies to reach the minimal point in  $\mathcal{R}_{III}$ , the attacker and the defender reach the point at the same time, as shown in Fig. 11(a). If

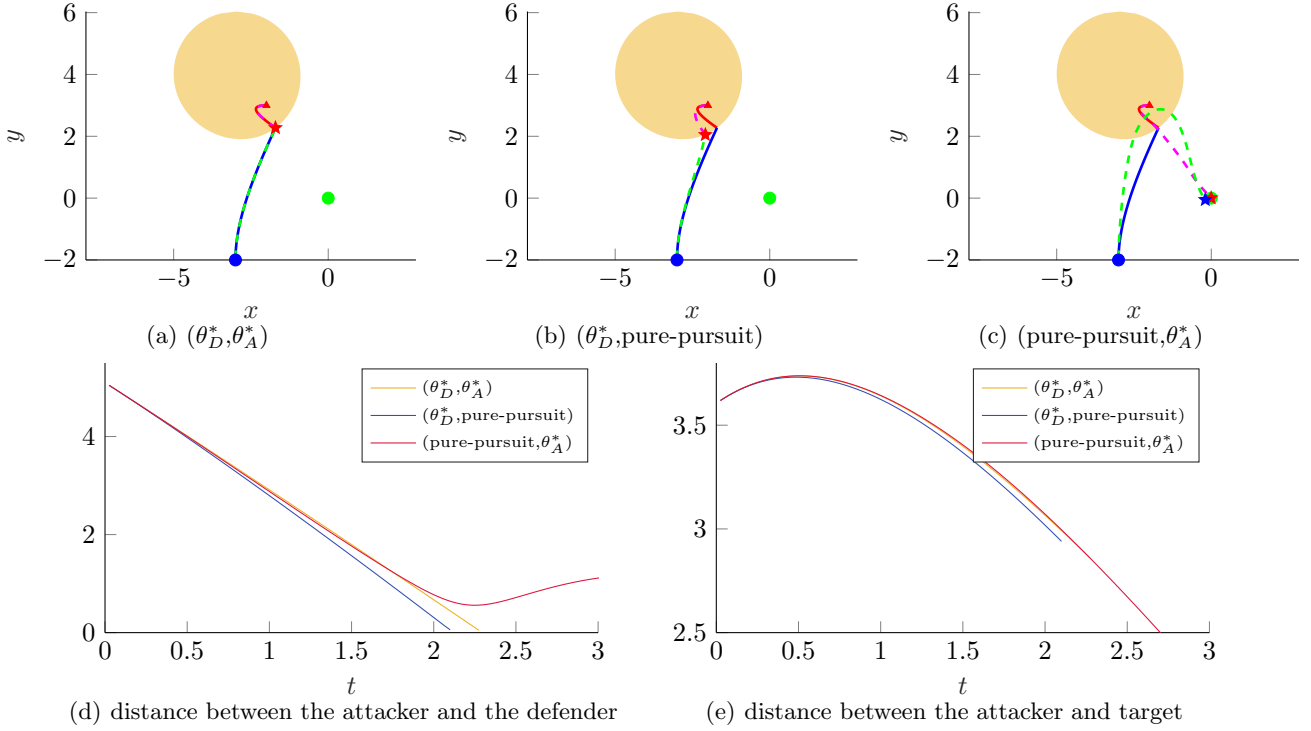


Fig. 7. Simulations of case 1. The trajectories of the attacker and defender applying open loop strategy I are red and blue lines, the attacker's and defender's trajectories of different strategies are pink and green dashed lines. The target is marked with green dot. (a) defender and attacker adopts strategy I. (b) defender adopts strategy I, attacker adopts pure-pursuit strategy. (c) the defender adopts pure-pursuit, attacker adopts strategy I. (d) distance between attacker and defender. (e) the distance between attacker and target.

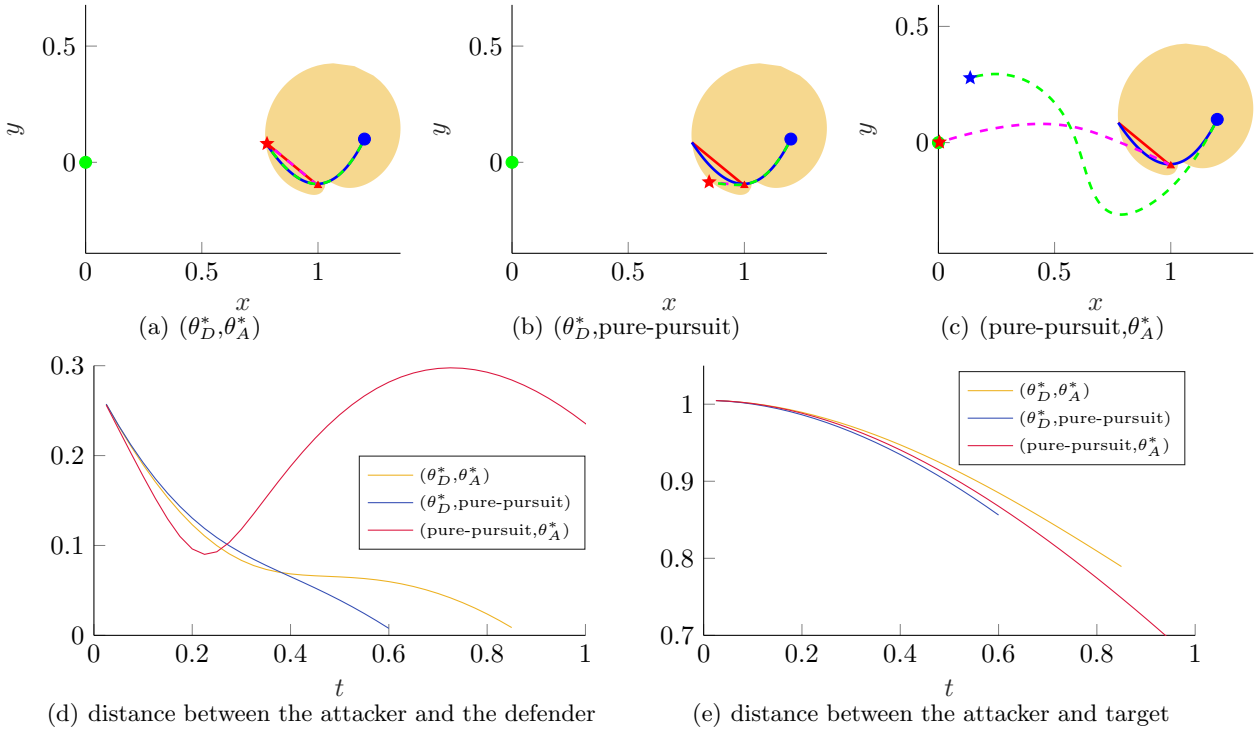


Fig. 8. Simulations of case 2.

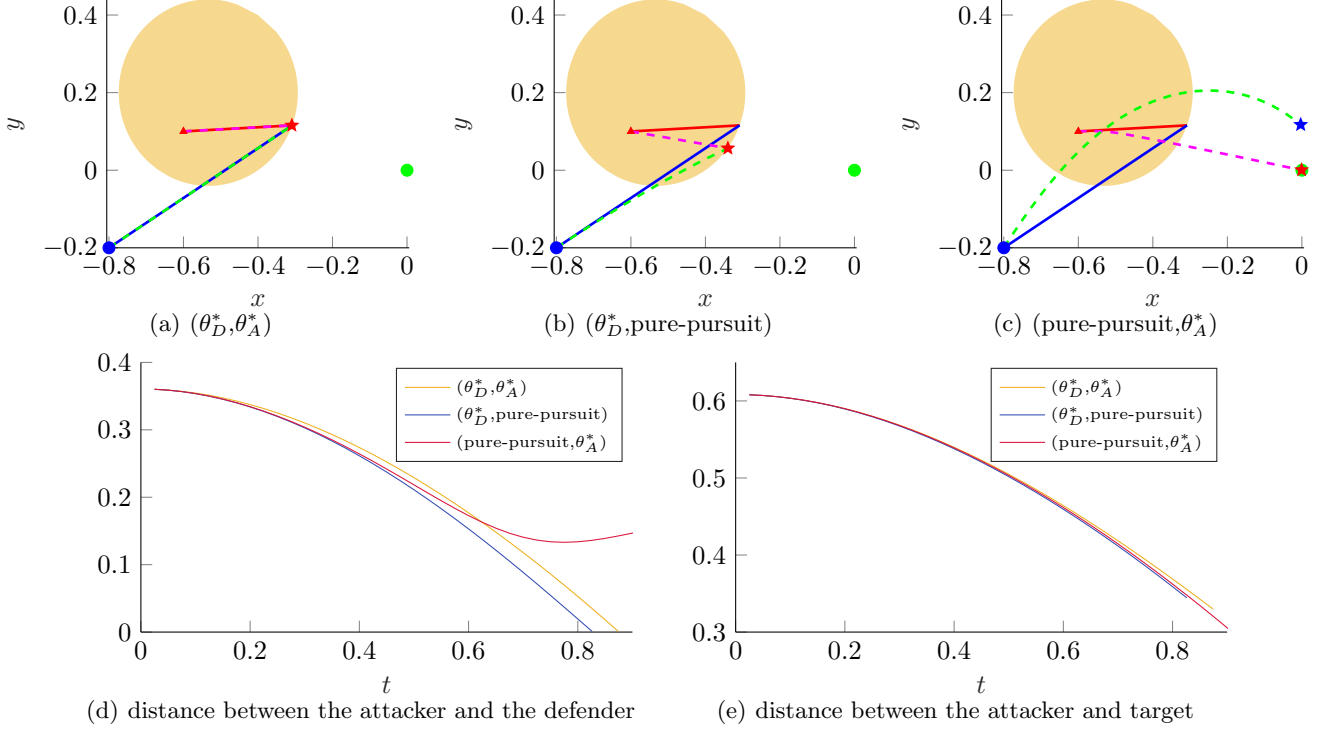


Fig. 9. Simulations of case 3. The initial velocity is 0 for the defender and attacker.

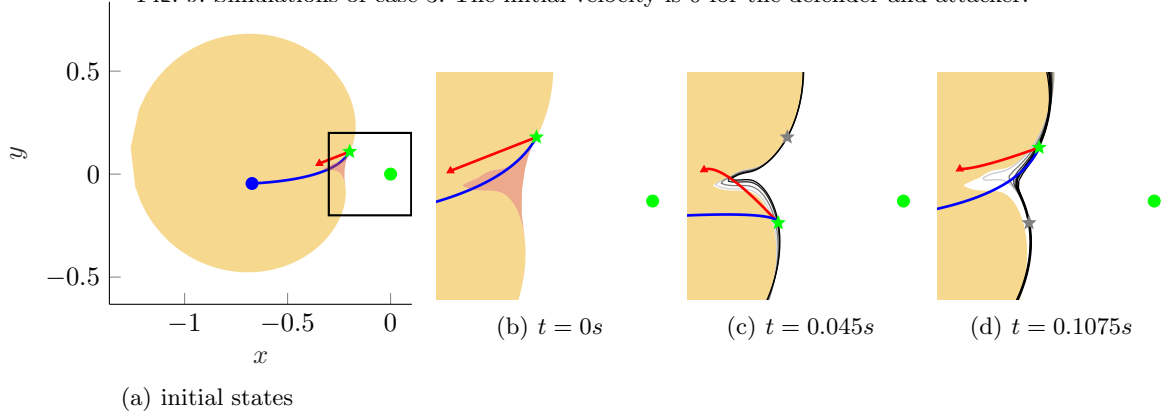


Fig. 10. Simulations of the special case 1 that the optimal point is in  $\mathcal{R}_{III}$ . The defender and attacker adopt strategy I. (a), (b) show the initial states and optimal point. (c) When  $t = 0.045s$ , the optimal point changes to another position, marked in green star, with the previous point in grey star. The boundaries of ADR from  $t = 0s$  to  $0.045s$  are curves in gray to black colors. (d) When  $t = 0.1075s$ , the optimal point changes again. The boundaries of ADR from  $t = 0.045s$  to  $0.1075s$  are curves in gray to black colors.

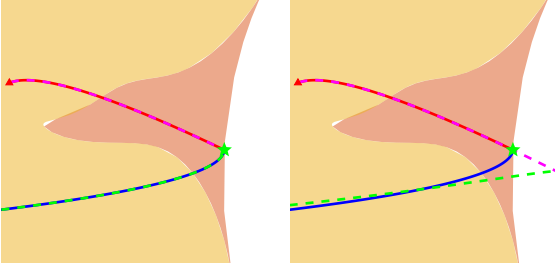
the defender still applies strategy I, the payoff function will become even smaller when the game terminates, as shown in Fig. 11(b).

In the second case, the minimal point is in  $\mathcal{R}_{II}$ . The attacker will apply strategy I while the defender aims to capture the attacker with strategy I in the shortest time, i.e. the defender's target point is the intersection of the attacker's trajectory and the boundary of  $\mathcal{R}_{III}$ . The initial states are set as follows:  $x_{A0} = 0$ ,  $y_{A0} = -5$ ,  $x_{D0} = -0.5$ ,  $y_{D0} = -4.9$ ,  $v_{Ax0} = 0$ ,  $v_{Ay0} = 0$ ,  $v_{Dx0} = 2$ ,  $v_{Dy0} = 0$ . The results of the game are shown in Fig. 12. Strategy I ne-

glects the possibility of being captured, resulting in the attacker being captured before arriving at the expected terminal point.

## 5 Conclusion

In this article, a reach avoid differential game with two damped double integrator players has been addressed. We first employed the Maximum Principle to investigate the properties of the optimal strategy. Then, we analyzed the multiple reachable region and isochrones of the players, presenting an algorithm to calculate isochrone circum-



(a) the attacker and the defender reach terminal strategy I point in  $\mathcal{R}_{III}$

Fig. 11. Simulations of the special case 1 that the optimal point is in  $\mathcal{R}_{III}$ . (a) The attacker and defender adopt strategies to reach the optimal point in  $\mathcal{R}_{III}$ . (b) The defender adopts strategy I, resulting in worse payoff for the defender.

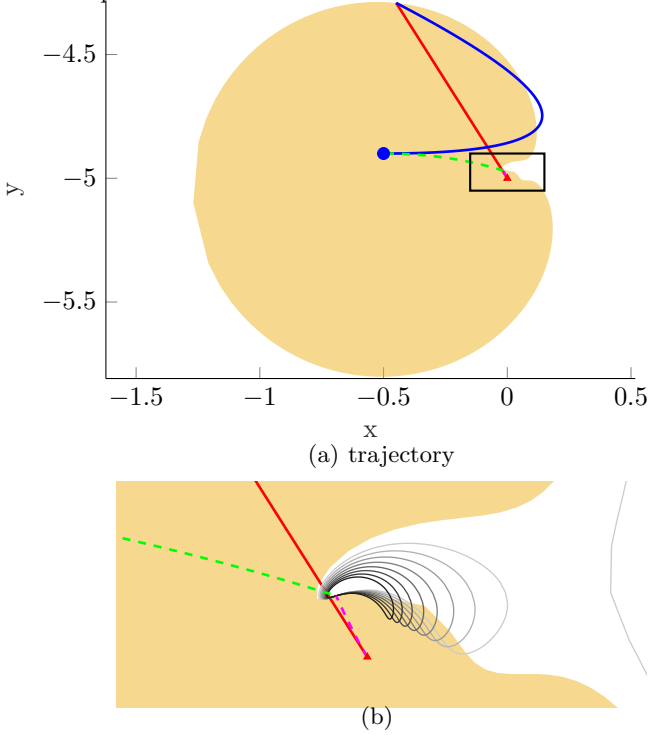


Fig. 12. Simulations of the special case 2 that the attacker has to cross  $\mathcal{R}_{III}$  to reach the optimal point in  $\mathcal{R}_{II}$ . The attacker adopts strategy I, while the defender tries to capture the attacker as soon as possible. As a result, the attacker is captured before reaching the optimal point. The boundaries of ADR at different times are curves with colors from grey to black.

scribe and inscribe times. We highlighted that the attacker's dominance region has distinct properties compared to other dynamic models, such as simple motion. Our proposed method to construct the attacker's dominance region utilizes isochrones and defender's multiple reachable region. As a result, the attacker's dominance region is categorized into three different types. Strategies to reach certain parts in the attacker's dominance region are provided. Additionally, we conducted simulations to demonstrate the performance of proposed

strategies across various scenarios.

In future work, we will focus on developing the strategy to reach the second type attacker's dominance region. In addition, since the dominance region is not convex, we will explore the situations involving multiple minimal points. Other methods such as using retrogressive path equations also worth further investigation.

## A Proof of Lemma 3

*Proof of Lemma 3.* Let  $\mathbf{v}_i(t) = \mathbf{v}_{i0}e^{-\mu t} + \mathbf{q}(t)$ , where  $\mathbf{q}(t) = [q_x(t), q_y(t)]^T$  satisfies

$$\begin{aligned} \dot{q}_x(t) &= -\mu q_x(t) + u_i(t) \cos \theta_i(t), \\ \dot{q}_y(t) &= -\mu q_y(t) + u_i(t) \sin \theta_i(t), \\ q_x(0) &= 0, \quad q_y(0) = 0, \end{aligned} \quad (49)$$

with  $u_i(t) < u_{im}$ . The trajectory of the player is given by:

$$\mathbf{x}_i(t) = \mathbf{x}_{i0} + \frac{\mathbf{v}_{i0}}{\mu}(1 - e^{-\mu t}) + \int_0^t \mathbf{q}(\tau) d\tau. \quad (50)$$

Then we have

$$\|\mathbf{x}_i(t) - \mathbf{x}_{ic}(t)\|_2 = \left\| \int_0^t \mathbf{q}(\tau) d\tau \right\|_2 \leq \int_0^t \|\mathbf{q}(\tau)\|_2 d\tau. \quad (51)$$

According to (49),

$$\dot{q}_x(t)^2 + \dot{q}_y(t)^2 + 2\mu \|\mathbf{q}(t)\|_2 \frac{d\|\mathbf{q}(t)\|_2}{dt} + \mu^2 \|\mathbf{q}(t)\|_2^2 = u_i(t)^2. \quad (52)$$

We also have

$$\begin{aligned} \left( \frac{d\|\mathbf{q}(t)\|_2}{dt} \right)^2 &= \left( \frac{d\sqrt{q_x^2(t) + q_y^2(t)}}{dt} \right)^2 \\ &= \frac{q_x^2(t)\dot{q}_x^2(t) + 2q_x(t)\dot{q}_x(t)q_y(t)\dot{q}_y(t) + q_y^2(t)\dot{q}_y^2(t)}{q_x^2(t) + q_y^2(t)} \\ &= \dot{q}_x^2(t) + \dot{q}_y^2(t) \\ &\quad - \frac{q_y^2(t)\dot{q}_x^2(t) - 2q_x(t)\dot{q}_x(t)q_y(t)\dot{q}_y(t) + q_x^2(t)\dot{q}_y^2(t)}{q_x^2(t) + q_y^2(t)} \\ &= \dot{q}_x^2(t) + \dot{q}_y^2(t) - \frac{(q_y(t)\dot{q}_x(t) - q_x(t)\dot{q}_y(t))^2}{q_x^2(t) + q_y^2(t)}. \end{aligned} \quad (53)$$

By Substituting (53) into (52), we have:

$$\frac{d\|\mathbf{q}(t)\|_2}{dt} + \mu \|\mathbf{q}(t)\|_2 \leq u_i(t).$$

According to Gronwall-Bellman Inequality,  $\|\mathbf{q}(t)\|_2 \leq \frac{u_{im}}{\mu}(1 - e^{-\mu t})$ . Substituting this into (51) yields

$$\|\mathbf{x}_i(t) - \mathbf{x}_{ic}(t)\|_2 \leq \int_0^t \frac{u_{im}}{\mu}(1 - e^{-\mu\tau})d\tau = r_{ic}(t). \quad (54)$$

Therefore, a player can only reach the points inside the isochron at  $t$ .

And for any point  $\mathbf{x}$  inside an isochron at  $t$ , the player can reach it by reducing the amplitude of acceleration to  $\hat{u}_i = \frac{\mu}{t - \frac{1 - e^{-\mu t}}{\mu}} \|\mathbf{x}_{ic}(t) - \mathbf{x}\|_2$ .  $\square$

## B Proof of Theorem 1

*Proof of Theorem 1.* We will first prove the case of circumscribing. The condition of circumscribing can be expressed as  $o(t) - p(t) = 0$ , where

$$\begin{aligned} o(t) &= \|\Delta\mathbf{x}\|_2^2 + \frac{\|\Delta\mathbf{v}\|_2^2}{\mu^2}(1 - e^{-\mu t})^2 + 2\frac{1}{\mu}\Delta\mathbf{x}^T\Delta\mathbf{v}(1 - e^{-\mu t}), \\ p(t) &= \frac{(u_A + u_D)^2}{\mu^2}\left(t - \frac{1 - e^{-\mu t}}{\mu}\right)^2. \end{aligned} \quad (55)$$

Given  $\|\Delta\mathbf{x}\|_2 > 0$ , it is obvious that  $o(0) - p(0) > 0$  and  $o(+\infty) - p(+\infty) < 0$ . We analyse the number of zeros points of  $o - p$  by analysing their derivatives with respect to  $t$ .

$$\begin{aligned} o' &= 2e^{-\mu t}\left(\frac{\|\Delta\mathbf{v}\|_2^2}{\mu}(1 - e^{-\mu t}) + \Delta\mathbf{x}^T\Delta\mathbf{v}\right), \\ o'' &= 2e^{-\mu t}(\|\Delta\mathbf{v}\|_2^2(2e^{-\mu t} - 1) - \mu\Delta\mathbf{x}^T\Delta\mathbf{v}), \\ o^{(3)} &= 2\mu e^{-\mu t}(\mu\Delta\mathbf{x}^T\Delta\mathbf{v} - \|\Delta\mathbf{v}\|_2^2(4e^{-\mu t} - 1)), \\ p' &= 2\frac{(u_A + u_D)^2}{\mu^2}\left(t - \frac{1 - e^{-\mu t}}{\mu}\right)(1 - e^{\mu t}), \\ p'' &= 2\frac{(u_A + u_D)^2}{\mu^2}\left(\left(1 - e^{-\mu t}\right)^2 + \mu e^{-\mu t}\left(t - \frac{1 - e^{-\mu t}}{\mu}\right)\right), \\ p^{(3)} &= 2\frac{(u_A + u_D)^2}{\mu^2}e^{-\mu t}(4(1 - e^{-\mu t}) - \mu t). \end{aligned} \quad (56)$$

The situation can be divided into 3 categories based on the monotonicity of  $o$ , which depends on  $\Delta\mathbf{x}^T\Delta\mathbf{v}$  and  $\|\Delta\mathbf{v}\|_2^2 + \mu\Delta\mathbf{x}^T\Delta\mathbf{v}$ .

**type 1:**  $\|\Delta\mathbf{v}\|_2^2 + \mu\Delta\mathbf{x}^T\Delta\mathbf{v} < 0$ . Since  $o' < 0, p' \geq 0$ ,  $o - p$  decreases monotonously and has only one zero point.

**type 2:**  $\|\Delta\mathbf{v}\|_2^2 + \mu\Delta\mathbf{x}^T\Delta\mathbf{v} \geq 0, \Delta\mathbf{x}^T\Delta\mathbf{v} \leq 0$ . We first investigate the zero point number of  $o'' - p''$ .

$p''(t) \geq 0, \forall t \in \mathbb{R}$  and  $p''(0) = 0$ .  $o''(t) > 0$  for  $t \in [0, t_M)$  where  $t_M = \frac{1}{\mu} \ln \frac{2\|\Delta\mathbf{v}\|_2^2}{\|\Delta\mathbf{v}\|_2^2 + \mu\Delta\mathbf{x}^T\Delta\mathbf{v}}$ .  $o''$  decrease

monotonously when  $t < t_M$ . We only consider  $t < t_M$  since only in this period could  $o'' - p'' = 0$

If  $o'' - p''$  has more than one zero point, then the following statement holds:

$$\exists t_1 < t_2 < t_M, \text{ s.t. } o''(t_1) - p''(t_1) < 0, o''(t_2) - p''(t_2) > 0.$$

According to Lagrange's mean value theorem, there exists a time  $t_3$  such that  $t_1 < t_3 < t_2, p^{(3)}(t_3) < o^{(3)}(t_3) < 0$ . The expression for the ratio is given by:

$$\frac{p^{(3)}}{o^{(3)}} = \frac{\frac{(u_A + u_D)^2}{\mu^2}(4(1 - e^{-\mu t}) - \mu t)}{\mu(\|\Delta\mathbf{v}\|_2^2 + \mu\Delta\mathbf{x}^T\Delta\mathbf{v} - 4\|\Delta\mathbf{v}\|_2^2 e^{-\mu t})}$$

The denominator increases monotonously, while the numerator decreases monotonously when  $p^{(3)}(t) < 0$ . Therefore,  $p^{(3)}(t) < o^{(3)}(t), \forall t > t_3$ . This implies that

$$p''(t) < o''(t), \forall t > t_2,$$

which is contradict to the fact that

$$p''(t_M) > o''(t_M).$$

Hence, there is only one zero point for  $o'' - p''$ .

This implies that  $o' - p'$  initially increases from  $2\Delta\mathbf{x}^T\Delta\mathbf{v}$  and then decreases to  $-\infty$ . There are at most two zeros points for  $o' - p'$ , denoted as  $t_{o1}, t_{o2}$ . So, the function  $o - p$  decreases for  $t < t_{o1}$ , increases for  $t_{o1} < t < t_{o2}$ , and decreases again for  $t > t_{o2}$ , having at most three zero points.

**type 3:**  $\Delta\mathbf{x}^T\Delta\mathbf{v} > 0$ .

We will first prove that  $o' - p'$  has only one zero point.

If  $\|\Delta\mathbf{v}\|_2^2 \leq \mu\Delta\mathbf{x}^T\Delta\mathbf{v}$ , then  $o''(t) < 0, \forall t$ , which means  $o' - p'$  decreases monotonously from  $2\Delta\mathbf{x}^T\Delta\mathbf{v}$  to  $-\infty$ .

If  $\|\Delta\mathbf{v}\|_2^2 > \mu\Delta\mathbf{x}^T\Delta\mathbf{v}$ , it is necessary to determine the number of zeros points of  $o'' - p''$ . The value of  $p^{(3)}$  at  $t_M$  is given by:

$$\begin{aligned} p^{(3)}(t_M) &= \\ &= 2\frac{(u_A + u_D)^2}{\mu^2}e^{-\mu t} \left( \frac{2\|\Delta\mathbf{v}\|_2^2 - \mu\Delta\mathbf{x}^T\Delta\mathbf{v}}{\|\Delta\mathbf{v}\|_2^2} \right. \\ &\quad \left. - \ln \frac{2\|\Delta\mathbf{v}\|_2^2}{\|\Delta\mathbf{v}\|_2^2 + \mu\Delta\mathbf{x}^T\Delta\mathbf{v}} \right). \end{aligned} \quad (57)$$

Let  $k = \frac{\mu\Delta\mathbf{x}^T\Delta\mathbf{v}}{\|\Delta\mathbf{v}\|_2^2} \in (0, 1)$ , the expression can be simplified to  $p^{(3)}(t_M) = 2\frac{(u_A + u_D)^2}{\mu^2}e^{-\mu t}(2(1 - k) + \ln \frac{1+k}{2})$ .

Since  $2(1-k) + \ln \frac{1+k}{2} > 0$  for  $k \in (0, 1)$ ,  $p^{(3)}(t_M) > 0$ . This implies that  $p''$  increases for  $t < t_M$ . So,  $o'' - p''$  only has one zero point.

The function  $o' - p'$  initially increases from  $2\Delta\mathbf{x}^T\Delta\mathbf{v}$ , during which it does not intersect with  $x = 0$ . It then decreases to  $-\infty$ . Hence,  $o' - p'$  has one zero point.

Therefore,  $o - p$  initially increases from  $\|\Delta\mathbf{x}\|_2^2$  and then decreases to  $-\infty$ , hence has one zero point.

The inscribe situation can be proven similarly.  $\square$

## References

- [1] Mo Chen, Jennifer C. Shih, and Claire J. Tomlin. Multi-vehicle collision avoidance via hamilton-jacobi reachability and mixed integer programming. In *2016 IEEE 55th Conference on Decision and Control (CDC)*, pages 1695–1700, 2016.
- [2] Eloy Garcia, David W Casbeer, and Meir Pachter. The complete differential game of active target defense. *Journal of Optimization Theory and Applications*, pages 1–25, 2021.
- [3] Xiaoming Duan, Mishel George, and Francesco Bullo. Markov chains with maximum return time entropy for robotic surveillance. *IEEE Transactions on Automatic Control*, 65(1):72–86, 2019.
- [4] Rufus Isaacs. *Differential games: a mathematical theory with applications to warfare and pursuit, control and optimization*. Courier Corporation, 1999.
- [5] Michael Dorothy, Dipankar Maity, Daigo Shishika, and Alexander Von Moll. One apollonius circle is enough for many pursuit-evasion games. *Automatica*, 163:111587, 2024.
- [6] Goutam Das, Michael Dorothy, Zachary I Bell, and Daigo Shishika. Defending a static target point with a slow defender. In *2024 American Control Conference (ACC)*, pages 4064–4071. IEEE, 2024.
- [7] Daigo Shishika and Vijay Kumar. Perimeter-defense game on arbitrary convex shapes. *arXiv preprint arXiv:1909.03989*, 2019.
- [8] Rui Yan, Zongying Shi, and Yisheng Zhong. Construction of the barrier for reach-avoid differential games in three-dimensional space with four equal-speed players. In *2019 IEEE 58th Conference on Decision and Control (CDC)*, pages 4067–4072. IEEE, 2019.
- [9] Elijah S Lee, Daigo Shishika, and Vijay Kumar. Perimeter-defense game between aerial defender and ground intruder. In *2020 59th IEEE conference on decision and control (CDC)*, pages 1530–1536. IEEE, 2020.
- [10] Keyang Wang, Shaobo Zhou, Yao Yao, Qi Sun, and Yintao Wang. A target defence-intrusion game with considering the obstructive effect of target. *IET Control Theory & Applications*, 2024.
- [11] Dave W Oyler, Pierre T Kabamba, and Anouck R Girard. Pursuit-evasion games in the presence of obstacles. *Automatica*, 65:1–11, 2016.
- [12] Rui Yan, Shuai Mi, Xiaoming Duan, Jintao Chen, and Xiangyang Ji. Pursuit winning strategies for reach-avoid games with polygonal obstacles. *IEEE Transactions on Automatic Control*, pages 1–16, 2024.
- [13] Eloy Garcia, David W Casbeer, and Meir Pachter. Escape regions of the active target defense differential game. In *Dynamic Systems and Control Conference*, volume 57243, page V001T03A001. American Society of Mechanical Engineers, 2015.
- [14] Eloy Garcia, David W Casbeer, and Meir Pachter. Escape regions of the active target defense differential game. In *Dynamic Systems and Control Conference*, volume 57243, page V001T03A001. American Society of Mechanical Engineers, 2015.
- [15] Eloy Garcia, David W Casbeer, Zachariah E Fuchs, and Meir Pachter. Aircraft defense differential game with non-zero capture radius. *IFAC-PapersOnLine*, 50(1):14200–14205, 2017.
- [16] Li Liang, Fang Deng, Zhihong Peng, Xinxing Li, and Wenzhong Zha. A differential game for cooperative target defense. *Automatica*, 102:58–71, 2019.
- [17] Alexander Von Moll, Meir Pachter, Daigo Shishika, and Zachariah Fuchs. Guarding a circular target by patrolling its perimeter. In *2020 59th IEEE conference on decision and control (CDC)*, pages 1658–1665. IEEE, 2020.
- [18] Daigo Shishika and Vijay Kumar. Local-game decomposition for multiplayer perimeter-defense problem. In *2018 IEEE conference on decision and control (CDC)*, pages 2093–2100. IEEE, 2018.
- [19] Daigo Shishika, James Paulos, and Vijay Kumar. Cooperative team strategies for multi-player perimeter-defense games. *IEEE Robotics and Automation Letters*, 5(2):2738–2745, 2020.
- [20] Rui Yan, Zongying Shi, and Yisheng Zhong. Reach-avoid games with two defenders and one attacker: An analytical approach. *IEEE transactions on cybernetics*, 49(3):1035–1046, 2018.
- [21] Eloy Garcia, Alexander Von Moll, David W Casbeer, and Meir Pachter. Strategies for defending a coastline against multiple attackers. In *2019 IEEE 58th conference on decision and control (CDC)*, pages 7319–7324. IEEE, 2019.
- [22] Ruiliang Deng, Zongying Shi, and Yisheng Zhong. Reach-avoid games with two cooperative attackers: Value function and singular surfaces. *IEEE Transactions on Aerospace and Electronic Systems*, 2023.
- [23] Mo Chen, Zhengyuan Zhou, and Claire J Tomlin. Multiplayer reach-avoid games via low dimensional solutions and maximum matching. In *2014 American control conference*, pages 1444–1449. IEEE, 2014.
- [24] Rui Yan, Xiaoming Duan, Zongying Shi, Yisheng Zhong, and Francesco Bullo. Matching-based capture strategies for 3d heterogeneous multiplayer reach-avoid differential games. *Automatica*, 140:110207, 2022.
- [25] Mo Chen, Zhengyuan Zhou, and Claire J. Tomlin. Multiplayer reach-avoid games via pairwise outcomes. *IEEE Transactions on Automatic Control*, 62(3):1451–1457, 2017.
- [26] Rui Yan, Zongying Shi, and Yisheng Zhong. Task assignment for multiplayer reach-avoid games in convex domains via analytical barriers. *IEEE Transactions on Robotics*, 36(1):107–124, 2019.
- [27] Ubaldo Ruiz. Capturing a differential drive robot with a dubins car. *IEEE Access*, 11:42124–42134, 2023.
- [28] Ubaldo Ruiz. Capturing a dubins car with a differential drive robot. *IEEE Access*, 10:81805–81815, 2022.
- [29] AW Merz. The game of two identical cars. *Journal of Optimization Theory and Applications*, 9:324–343, 1972.

- [30] Luis Bravo, Ubaldo Ruiz, and Rafael Murrieta-Cid. A pursuit–evasion game between two identical differential drive robots. *Journal of the Franklin Institute*, 357(10):5773–5808, 2020.
- [31] Mitchell Coon and Dimitra Panagou. Control strategies for multiplayer target-attacker-defender differential games with double integrator dynamics. In *2017 IEEE 56th Annual Conference on Decision and Control (CDC)*, pages 1496–1502. IEEE, 2017.
- [32] Wei Yongshang, Liu Tianxi, and Wei Cheng. Winning region determination and optimal cooperative guidance design in a pursuer–evader–defender game. *Dynamic Games and Applications*, pages 1–16, 2024.
- [33] Eloy Garcia, David W. Casbeer, and Meir Pachter. Active target defense using first order missile models. *Automatica*, 78:139–143, 2017.
- [34] Shuai Li, Chen Wang, and Guangming Xie. Optimal strategies for pursuit-evasion differential games of players with damped double integrator dynamics. *IEEE Transactions on Automatic Control*, 2023.